AD-A185 937 THEORY OF LOW-TEMPERATURE ADSORPTION(U) STATE UNIV OF NEW YORK AT BUFFALO DEPT OF CHEMISTRY S G CHUNG ET AL. SEP 87 UBUFFALO/DC/87/TR-49 N00014-86-0043 1/1

UNCLASSIFIED F/G 7/4 NL

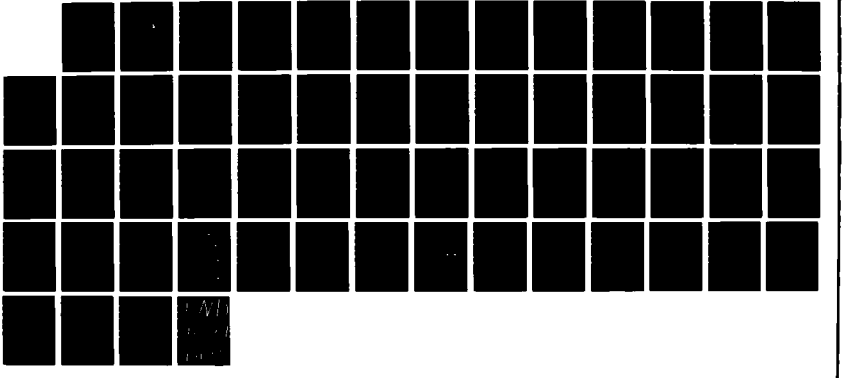

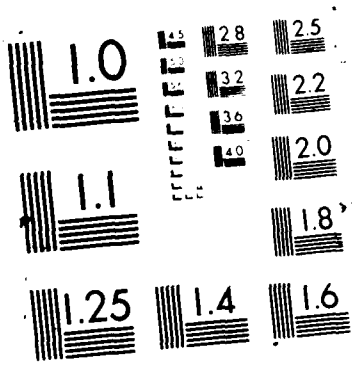
1.0
1.1
1.25
2.8
3.2
3.6
4.0
2.5
2.2
2.0
1.8
1.4
1.6

(12)

OFFICE OF NAVAL RESEARCH

Contract N00014-86-0043

TECHNICAL REPORT No. 51

Theory of Low-Temperature Adsorption

by

S. G. Chung and Thomas F. George

Prepared for Publication

in

Surface Science

Departments of Chemistry and Physics
State University of New York at Buffalo
Buffalo, New York 14260

September 1987

UNCLASSIFIED

SECURITY CLASSIFICATION OF THIS PAGE

REPORT DOCUMENTATION PAGE

1a. REPORT SECURITY CLASSIFICATION Unclassified	1b. RESTRICTIVE MARKINGS
2a. SECURITY CLASSIFICATION AUTHORITY	3. DISTRIBUTION/AVAILABILITY OF REPORT Approved for public release; distribution unlimited
2b. DECLASSIFICATION/DOWNGRADING SCHEDULE	
4. PERFORMING ORGANIZATION REPORT NUMBER(S) UBUFFALO/DC/87/TR-49	5. MONITORING ORGANIZATION REPORT NUMBER(S)
6a. NAME OF PERFORMING ORGANIZATION Depts. Chemistry & Physics State University of New York 6b. OFFICE SYMBOL (If applicable)	7a. NAME OF MONITORING ORGANIZATION
6c. ADDRESS (City, State and ZIP Code) Fronczak Hall, Amherst Campus Buffalo, New York 14260	7b. ADDRESS (City, State and ZIP Code) Chemistry Program 800 N. Quincy Street Arlington, Virginia 22217
8a. NAME OF FUNDING/SPONSORING ORGANIZATION Office of Naval Research 8b. OFFICE SYMBOL (If applicable)	9. PROCUREMENT INSTRUMENT IDENTIFICATION NUMBER Contract N00014-86-0043
8c. ADDRESS (City, State and ZIP Code) Chemistry Program 800 N. Quincy Street Arlington, Virginia 22217	10. SOURCE OF FUNDING NOS. PROGRAM ELEMENT NO. / PROJECT NO. / TASK NO. / WORK UNIT NO.
11. TITLE Theory of Low-Temperature Adsorption	
12. PERSONAL AUTHOR(S) S. G. Chung and Thomas F. George	
13a. TYPE OF REPORT 13b. TIME COVERED FROM _____ TO _____	14. DATE OF REPORT (Yr., Mo., Day) September 1987 15. PAGE COUNT 51
16. SUPPLEMENTARY NOTATION Prepared for publication in Surface Science	
17. COSATI CODES FIELD / GROUP / SUB. GR.	18. SUBJECT TERMS (Continue on reverse if necessary and identify by block number) LOW-TEMPERATURE ADSORPTION; SMALL WAVE NUMBER LIMIT THEORY; MORSE-TYPE POTENTIALS; QUANTUM STICKING COEFFICIENT; INVERSE-SQUARE POTENTIALS

19. ABSTRACT (Continue on reverse if necessary and identify by block number)

A general and qualitatively exact theory is developed for quantum sticking coefficients $\alpha(k)$ in the small wave number limit, $k \to 0$. The theory covers Morse-type to inverse-square potentials, the latter representing long-range potentials. The theory gives unambiguous answers to crucial questions in the problem and helps lead to an overall understanding of low-temperature adsorption.

20. DISTRIBUTION/AVAILABILITY OF ABSTRACT UNCLASSIFIED/UNLIMITED ☒ SAME AS RPT. ☒ DTIC USERS ☐	21. ABSTRACT SECURITY CLASSIFICATION Unclassified
22a. NAME OF RESPONSIBLE INDIVIDUAL Dr. David L. Nelson	22b. TELEPHONE NUMBER (Include Area Code) (202) 696-4410 22c. OFFICE SYMBOL

DD FORM 1473, 83 APR EDITION OF 1 JAN 73 IS OBSOLETE.

UNCLASSIFIED

SECURITY CLASSIFICATION OF THIS PAGE

Surface Science, in press

THEORY OF LOW-TEMPERATURE ADSORPTION

S. G. Chung† and Thomas F. George

Departments of Chemistry and Physics & Astronomy
239 Fronczak Hall
State University of New York at Buffalo
Buffalo, New York 14260

Abstract

A general and qualitatively exact theory is developed for quantum sticking coefficients $\alpha(k)$ in the small wave number limit $k \to 0$. The theory covers Morse-type to inverse-square potentials, the latter representing long-range potentials. The theory gives unambiguous answers to crucial questions in the problem and helps lead to an overall understanding of low-temperature adsorption.

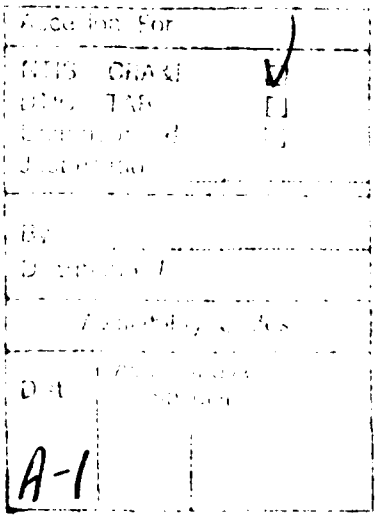

†Present address: Department of Physics, Western Michigan University, Kalamazoo, Michigan 49008

I. Introduction

The problem of determining sticking coefficients of an atom on material surfaces is one of the fundamental tasks in surface physics. A general situation is depicted in Fig. 1a. If the kinetic energy of incident atoms or molecules is large compared with the energy scale of the problem, e.g., a potential-well depth of matter-particle interaction, then it is widely believed that the distorted-wave-Born-approximation (DWBA) is quantitatively correct for describing various surface phenomena.[1,2] On the other hand, when the incident kinetic energy is much smaller than the typical energy scale of the given problem, as realized in low temperatures, there has been a long-standing controversy concerning the validity of the DWBA.[3-7] This is partly due to the lack of accurate experiments at small k and at low temperatures. The only exception is the experiment done by the Edward group.[8]

The present theoretical situation is the following. People believe that a one-dimensional (1-d) simplification, as depicted in Fig. 1b, is good enough to study qualitative properties of the sticking coefficients $\alpha(k)$ at low temperatures. It is noted that a T-shape model as shown in Fig. 1c has a deficiency that there is no momentum sink along the direction of the particle motion. In classical mechanics, a particle would eventually strike the surface no matter how slow it is, releasing some energy to a matter system, and therefore, it would definitely be adsorbed on the surface for vanishingly small incident energy. Quantum mechanically, however, the situation is not quite so obvious. First, it appears natural that in quantum mechanics a low-energy wave function of the atom must have a small wave amplitude at a high potential barrier, i.e., at a surface. This is true for static short-range potentials due to the following reason. Consider a static square-well potential as shown in Fig. 2. The scattering wave function with incident wave number k can be written as

$$|k^+\rangle = \begin{cases} A \sin(Kx) & \text{for } 0 \leq x \leq R \\ e^{-ikx} - S(k)e^{ikx} & \text{for } R < x \end{cases} , \tag{1.1}$$

where S(k) is an S-matrix element and

$$\frac{\hbar^2 K^2}{2m} = \frac{\hbar^2 k^2}{2m} + D , \tag{1.2}$$

where m is the particle mass. Imposing the smoothness condition on $|k^+\rangle$ at $x = R$, one can easily find that

$$A \propto k , \quad S(k) \to 1 \quad \text{for } k \to 0 . \tag{1.3}$$

The linear k-dependence of the scattering wave amplitude in the potential-well region immediately leads to a linear k-dependence of the sticking coefficient $\alpha(k)$ at small k. The first quantum-mechanical calculation of $\alpha(k)$ by Lennard-Jones and Devonshire (LJD)[3] based on the DWBA is essentially the same as the above argument for the static square-well potential. Based on the LJD calculation for a static Morse potential which decays exponentially at large distance, people next considered various possible mechanisms for realizing finite $\alpha(0)$. These include static long-range potentials, x^{-n},[7] and correlated or many-body motions of the atom-matter system such as polaron[6] and self-trapping,[5] but for short-range potentials like square-well and Morse-type. However, all the existing theories share a common deficiency in that they do not answer the following two questions: How important is the long-range character of the matter-particle interaction? How important is the many-body motion of the matter-particle system? It is clear that a satisfactory theory must treat these effects on an equal-footing. Are there any potentials for which $\alpha(0)$ are finite? If there are such potentials, what is a borderline potential which distinguishes between "short-range" potentials for which $\alpha(0) = 0$ and "long-range" potentials for which $\alpha(0) \neq 0$?

In this paper, we shall develop a new theory of quantum sticking coefficients at 0 K. We do not invoke any uncontrolled approximations, and thus give a definitive answer to the problem. Our answer is as follows: (i) Irrespective of the matter-particle interaction potentials, the many-body motion of matter-particle system is not essential for the small-k behavior of $\alpha(k)$. The present theory gives a firm basis to the DWBA. (ii) For potentials decaying faster than x^{-2} at large distance, $\alpha(k) \propto k$ at small k. This is essentially due to the fact that the scattering wave function has a linear k-dependence at small k. The range of the linear k region decreases with increasing long-range character of the matter-particle interactions. The theory encourages experiments at small $k \lesssim 0.1$ Å^{-1}. For a ^{4}He atom colliding with a liquid ^{4}He surface, the present theory predicts a critical wave number ~ 0.01 Å^{-1} below which $\alpha(k)$ depends on k approximately linearly, which provides a deep understanding of the experiment.[8] (iii) The inverse-square potential is a borderline distinguishing between short-range potentials for whish $\alpha(0) = 0$ and long-range potentials for which $\alpha(0) \neq 0$. This conclusion is reached by a DWBA calculation of $\alpha(k)$ for the inverse square potential. Our assertion (i) in this case means that the DWBA result cannot be changed qualitatively by higher-order corrections. This is essentially due to the fact that, unlike the case of short-range potentials, the scattering wave function here has a $\sqrt{k}$-singularity at small k.

Before getting into detailed descriptions, let us try an intuitive explanation of the present theory and its main results. To do so, consider once more the static square-well potential, Fig. 2. In the above, we have given a standard explanation of $\alpha(0) = 0$. Our method in this simple case would proceed as follows. We first note that the S-matrix element $S(k) = \exp[2i\delta(k)]$, where $\delta(k)$ is a scattering phase shift. But Levinson's theorem[9] tells us that $\delta(k)$ is related to the number of bound state N of the square-well potential as

$$\delta(+0) = \pi N \quad . \tag{1.4}$$

Now for $k \ll 1$, $S(k) \sim 1$ by (1.4) and $R \sim 0(1)$ for short-range potentials, and therefore

$$|k^+\rangle \simeq -2ikx \quad \text{for} \quad R < x \ll 1/k \quad . \tag{1.5}$$

On the other hand, $|k^+\rangle$ in the region $0 \leq x \leq R$ must be a linear combination of two independent solutions of the Schrödinger equation, $e^{\pm iKx}$. Noting that K does not depend on k in the limit $k \to 0$, and requiring a smooth connection of $|k^+\rangle$ at $x = R$, one can easily see that both two constant factors before $e^{\pm iKx}$ are proportional to k, which leads to the same result as before -- $|k^+\rangle \propto k$ at the potential well, and hence $\alpha(k) \propto k$ for small k. Now the point is, this explanation does not use the boundary condition at $x = 0$, nor does it require details of the wave function in the potential well. Therefore, under the existence of a dynamical version of Levinson's theorem, it can be extended to dynamical cases, which is precisely what we shall do in the next section. The existence of a dynamical version of Levinson's theorem for matter-particle interaction potentials decaying faster than x^{-2} has recently been shown by the present authors.[10]

We have organized the present paper as follows. In the next section, short-range potentials are examined based on formal scattering theory and the dynamical Levinson's theorem. In Section III, a numerical calculation of $\alpha(k)$ is carried out based on a self-trapping model, which demonstrates the dynamical Levinson's theorem and determines a standard number β to be introduced in Section II. In Section IV, we examine the inverse square potential which is essentially different from the short-range cases and is outside the scope of the arguments to be presented in Section II. Our DWBA calculation presents, for the first time, an example of finite $\alpha(0)$. Our summary is given in Section V.

(After the completion of the present work, we have noticed the paper by Brivio and Brimley in which the adsorption problem is treated by the Green's function method.[21])

II. Short-Range Potentials

We first examine short-range potentials, that is, those decaying faster than x^{-2}. Let us consider the adatom + 1-d matter Hamiltonian in a collinear configuration (see Fig. 1b),

$$H_{tot} = H(\tilde{x},\tilde{p}) + V(\tilde{x},x) + K(p) \quad , \tag{2.1}$$

where $H(\tilde{x},\tilde{p})$ is a 1-d matter Hamiltonian with $\tilde{x}$ and $\tilde{p}$, respectively, representing position and momentum vectors for atoms in the 1-d matter, $V(\tilde{x},x)$ is an interaction potential between the adatom and 1-d matter which we restrict to those decaying faster than x^{-2} at large adatom-matter separation $x >> 1$, and $K(p)$ is the kinetic energy of adatom. It is noted that the 1-d matter must be of finite size, because otherwise only one phase is possible in one dimension, that is, there is no distinction between gases, liquids and solids.[11] This means that the matter does not have a well-defined boundary at finite temperatures, and the question of calculating an adsorption probability becomes meaningless.

A scattering eigenstate of (2.1) with a wave number k can be written as

$$\psi(\tilde{r},k) = F(\tilde{r},k) - S(k)F(\tilde{r},-k) \quad , \tag{2.2}$$

where $\tilde{r} \equiv (\tilde{x},x)$, $F(\tilde{r},k)$ is a Jost solution having an asymptotic form $e^{-ikx}\phi_0(\tilde{x})$ at $x \to \infty$, where $\phi_0(\tilde{x})$ is the ground state of $H(\tilde{x},\tilde{p})$ (T = 0 K), and $S(k) = \exp[2i\delta(k)]$ is an S-matrix element. In a recent paper,[10] we have extended Levinson's theorem in static potential scattering to our dynamical case. We

have shown that for our short-range potential $V(\tilde{x},x)$, the scattering phase shift $\delta(k)$ is connected to the number of bound states, N, of the total Hamiltonian by

$$\delta(+0) = N\pi \quad . \tag{2.3}$$

On the other hand, an exact expression of an adsorption rate R(k), the number of adsorped atoms per unit time, is given by time-dependent scattering theory[12] as

$$R(k) = \frac{2\pi}{\hbar} \sum_f \delta(E_k - E_f) |\langle f|V_f|k^+\rangle|^2 \quad , \tag{2.4}$$

where $E_k = \frac{\hbar^2 k^2}{2m} + E_0$ with E_0 representing the ground state energy of the matter (T = 0 K), $\sum_f$ means a summation over final states $|f\rangle$, V_f is a final channel interaction, e.g., creation of phonons, and $|k^+\rangle$ represents a scattering eigenstate of the total Hamiltonian, H_{tot}. The sticking coefficient $\alpha(k)$ is defined as a ratio between R(k) and the flux, the number of incident atoms per unit time, which is given by $\hbar k/m$. Therefore we have

$$\alpha(k) = \frac{2\pi m}{\hbar^2 k} \sum_f \delta(E_k - E_f) |\langle f|V_f|k^+\rangle|^2 \quad . \tag{2.5}$$

An important observation in (2.5) is that as far as the small-k behavior of $\alpha(k)$ is concerned, it is given essentially by the quantity $|k^+\rangle^2/k$. This is seen as follows. The static potential

$$V(\tilde{x}_0,x) = V(\tilde{x},x) - V_f \quad , \tag{2.6}$$

where $\tilde{x}_0$ denotes a mean configuration of matter atoms in the ground state $\phi_0(\tilde{x})$, is by assumption a short-range potential, and supports only a finite number of bound states with finite binding energies. Moreover, the final states $|f\rangle$ in

(2.5) are eigenstates of the unperturbed Hamiltonian $H_{tot}-V_f$. Therefore, in the limit $k \to 0$, all the quantities other than $|k^+>^2/k$ in (2.5) do not depend on k.

We now explore the small-k behavior of the exact scattering eigenstate $|k^+>$. From the dynamical Levinson's theorem (2.3), for $k \ll 1$ the S-matrix element $S(k) = \exp[2i\delta(k)] \sim 1$ in (2.2). Let us define a reduced potential

$$V(\tilde{x}_0,x)/(\frac{\hbar^2}{2m}) \equiv U(x) \quad . \tag{2.7}$$

and consider large distances R and R' such that

$$-U(R) = k^2 \ll -U(R') \ll \{-U(x)\}_{max} \quad . \tag{2.8}$$

This means that the matter system is still in the ground state in the region $R' < x$, and that the Jost solution in (2.2) is $F(\tilde{r},k) \equiv e^{-ikx}\phi_0(\tilde{x})$ in the region $R < x$. Thus we have

$$\begin{aligned} |k^+> &\equiv (e^{-ikx} - e^{ikx})\,\phi_0(\tilde{x}) \\ &\equiv -2ikx\phi_0(\tilde{x}) \quad \text{for} \quad R < x < \frac{1}{k} \quad , \end{aligned} \tag{2.9}$$

where in the second expression, we have assumed the inequality

$$kR < 1. \tag{2.10}$$

Next consider the region $R' < x < R$, where the particle motion is described by Schrödinger equation

$$\{-\frac{d^2}{dx^2} + U(x)\}\,\psi = k^2\psi \quad . \tag{2.11}$$

Instead of explicitly solving (2.11) for respective potentials U(x), however, we simply point out that the particle motion in this region must be somewhere between the two extreme cases, $U(x) = U(R)$ and $U(x) = U(R')$, as shown by two

horizontal dashed lines in Fig. 3. But one can easily see that in both cases the smoothness requirement of $|k^+\rangle$ at $x = R$ [cf. (2.9)] leads to $|k^+\rangle \propto k$ at $R' < x < R$. This fact in turn leads to $|k^+\rangle \propto k$ at $0 < x < R'$, because in this region, $|k^+\rangle$ can depend on k only through a constant prefactor which, however, again by smoothness of $|k^+\rangle$ at $x = R'$, must be proportional to k. In this way we reach

$$|k^+\rangle \propto k \qquad 0 < x < R. \tag{2.12}$$

From (2.12) we have

$$\alpha(k) \propto |k^+\rangle^2/k \propto k \quad . \tag{2.13}$$

We remember, however, that (2.13) is derived under the condition (2.10) and $S(k) \sim 1$. Little is known about the small-k dependence of S(k). Our analysis below and numerical calculations in the next section for a Morse potential show that the latter condition imposes a similar restriction on k as (2.10). To analyze (2.10) for typical long-distance behaviors of the reduced potential U(x), let us introduce a standard number $\beta < 1$ in analogy to the "standard value" in the Lindemann formula for melting,[13] and replace (2.10) by

$$kR \leq \beta \quad . \tag{2.14}$$

With this β we can predict for each given potential a critical wave number k_c such that

$$\alpha(k) \propto k \quad \text{at} \quad k \leq k_c \quad . \tag{2.15}$$

From (2.14) and $U(R) = k^2$, one can easily obtain the following results:

(i) Exponential decay $U(x) \sim -\gamma e^{-\kappa x}$,

$$-(k_c/\kappa)\ln(k_c^2/\gamma) = \beta \tag{2.16}$$

(ii) Algebraic decay $U(x) \sim -\gamma x^{-n}$ $(n > 2)$,

$$\gamma^{1/n} k_c^{1-2/n} = \beta \ . \tag{2.17}$$

The results (2.16) and (2.17) make two predictions. First, the critical wave number k_c decreases with increasing long-range character of the potential. Our numerical calculations of $\alpha(k)$ in the next section for a Morse potential (2.16) with $\gamma = 48$ Å^{-1} and $\kappa = 1.4$ Å^{-1} (numbers for the W-He system[14,15]) show that $k_c \sim 0.1$ Å^{-1}. Substituting these numbers into (2.16) gives

$$\beta \sim 0.6 \ . \tag{2.18}$$

The ^{4}He atom colliding on a liquid ^{4}He surface is described by a van der Waals potential (2.17) with $n = 3$ and $\gamma = 20$ Å. Using $\beta \sim 0.6$ in (2.17), we have $k_c \sim 0.01$ Å^{-1} for this case, which is in good agreement with experiment.[8] Second, from (2.17) k_c approaches zero quite rapidly as the exponent n approaches 2 from above, as depicted in Fig. 4 for $\gamma = 20$ and $\beta = 0.6$. This strongly suggests finite $\alpha(0)$ for an inverse square potential, and that $n = 2$ is a borderline distinguishing between "short-range" potentials $n > 2$ and "long-range" potentials $n \leq 2$. We note that the $n = 2$ specialty is beyond physical intuition, but is clear mathematically as signaled in several ways: the dynamical Levinson's theorem (2.3) breaks down for $n \leq 2$, the inequality (2.10) does not hold for $n \leq 2$, and the zero-energy scattering wave function has a singularity at $n = 2$. This last fact is seen as follows. For $k = 0$ and $U(x) = -\gamma x^{-n}$, (2.11) becomes

$$\psi'' + \gamma x^{-n}\psi = 0 \ . \tag{2.19}$$

A general solution of (2.19) is

$$\psi = \sqrt{x}\, Z_{\frac{1}{2-n}}\left(\frac{2\sqrt{\gamma}}{2-n}\, x^{1-n/2}\right) \quad , \tag{2.20}$$

where Z_ν is a solution of Bessel's differential equation

$$Z_\nu'' + \frac{1}{x} Z_\nu' + \left(1 - \frac{\nu^2}{x^2}\right) Z = 0 \quad . \tag{2.21}$$

The singularity of ψ at $n = 2$ is clear in (2.20). In Section IV, we shall present a thorough study of the inverse square potential and show that the quantum sticking coefficient $\alpha(k)$ is finite in the limit $k \to 0$, thus confirming the above prediction that $n = 2$ is a borderline.

III. Determination of β

In this section, we consider a self-trapping model for the adsorption of He atom on W. A collinear configuration of He and W is shown in Fig. 5. By calculating the sticking coefficient $\alpha(k)$ as a function of the wave number k, we shall demonstrate the dynamical Levinson's theorem (2.3) and determine the standard number β. The model assumes a harmonic lattice, $H_{ph} = \sum_q \hbar\omega_q a_q^\dagger a_q$, a surface W atom plus He atom interacting through a Morse potential, and the surface W atom seeing another Morse potential created by the end W atom of the 1-d lattice in its equilibrium (taken to be $x = 0$)

$$H_{s+a} = p_s^2/2M + \bar{U}(x_s) + p_a^2/2m + U(x_a - x_s) \quad . \tag{3.1}$$

The dynamical interaction between the harmonic lattice and the surface W atom takes the form (one-phonon process)

$$H_{int} = -\sum_q \left(\frac{\hbar}{2N_0 M\omega_q}\right)^{\frac{1}{2}} (a_q^\dagger + a_{-q}) \frac{d\bar{U}(x_s)}{dx_s}\, \theta(t) \quad , \tag{3.2}$$

where N_0 is the number of lattice atoms, and the unit step function $\theta(t)$ means that $|k^+\rangle$ here is a scattering eigenstate of H_{s+a}, not that of the total Hamiltonian. In analogy to the second-order optical process, this is a luminescence component approximation thereby neglecting Raman components, which is expected to be good for short-range potentials of the Morse type. To calculate $\alpha(k)$ by (2.5), we note that here V_f is H_{int} at $t > 0$, and the final state is $|f\rangle = a_q^\dagger|0\rangle|b\rangle$, where $|0\rangle$ is the phonon vacuum and $|b\rangle$ represents a bound state of H_{s+a}.

To solve the Schrödinger equation

$$H_{s+a}\psi = E\psi \quad , \tag{3.3}$$

which is the main task in this section, we now specify the W-He and W-W Morse potentials as

$$\begin{bmatrix} \bar{U}(x+x_s^0) \\ U(x+x_a^0) \end{bmatrix} = \begin{bmatrix} \bar{D} \\ D \end{bmatrix} (e^{-2\kappa x} - 2e^{-\kappa x}) \quad , \tag{3.4}$$

where $x_s^0 \sim 3$ Å, $x_a^0 \sim 3.6$ Å, $\bar{D} \sim 0.99$eV, $D \sim 10$ meV and $\kappa \cong 1.4$ Å^{-1}.[14,15] The phonon dispersion ω_q is given in terms of the W-W interaction potential $\bar{U}$ as

$$M\omega_q^2 = 2\bar{U}_{xx}(x=x_s^0)[1 - \cos(qx_s^0)] \quad . \tag{3.5}$$

It is worth noting that the problem (3.3) is essentially a three-body one and an analytic solution is not available even for the simplest interaction potentials, e.g., the square-well. The best we can do is to construct perturbative and variational wave functions and solve (3.3) numerically. In doing so, we note the following. First, the one-body problem for Morse potentials is exactly solvable. Appendix A summarizes some results about Morse potentials. In the case of the W-He Morse potential U(x), the quantity K as defined in (A.3) is

about 7.4, which by (A.6) means that there are four bound states with the lowest binding energy ~ -1.52×10^{-21} J ≈ -9 meV. Similarly for the W-W Morse potential $\bar{U}(x)$, there are about 200 bound states. Measuring the energy from that of the lowest bound state, the first four bound states have energies 0 (n = 0), 1.35 (n = 1), 2.69 (n = 2) and 3.94 (n = 3) in the unit of 10^{-21} J. The one-particle energy spectra for the W-W and W-He Morse potentials are schematically summarized in Fig. 6. It is now clear from energy considerations that as long as k is small, the first three bound states are good enough to describe the motion of the surface W-atom. As for the motion of He, there are two situations. When the He atom is far away from the surface, the surface W-atom is in the ground state and the wave function is written as

$$\psi = \psi_{asym}(x_s,x_a) = C\phi_0(x_s)[e^{-ikx_a} - S(k)e^{ikx_a}] \quad , \tag{3.6}$$

where $\phi_0(x_s)$ is the ground state of the surface w-atom as given by (A.2), and C = 0 for bound states $|b\rangle$ and C = 1 for the scattering state $|k^+\rangle$. Near the surface, on the other hand, the wave function can be written as

$$\psi = \psi_{surf}(x_s,x_a) = \sum_{p=0}^{M-1} g_p(x_a)\phi_p(x_s) \quad , \tag{3.7}$$

where the g_p's describe a fully correlated motion of He near the surface. According to the energy consideration above, we take M = 3 hereafter. One may suggest the use of the variable $x_a - x_s$ in place of x_a in (3.7) and expand the He motion g_p in terms of the eigenstates $\{\phi_n\}$ in (A.2) for the W-He Morse potential U. This scheme is not efficient, however, because of complexities arising from the kinetic energy term $p_s^2/2M$ in (3.1). We find that the Gaussian-weighted Hermite polynomials are the best suited orthonormal complete set over which to expand localized g_p-functions:

$$h_q = \tilde{N}_q e^{-T^2x^2/4} H_q(Tx) \qquad q = 0,1,2\ldots \quad , \tag{3.8}$$

where $\tilde{N}_q = [T/q!\sqrt{2\pi})]^{1/2}$ and the H_q's are Hermite polynomials. In Appendix B, we have described Hermite polynomials and related integrals which appear in the calculation of the Hamiltonian matrix elements. The scale factor T in (3.8) must be best fitted according to the degree of locality of the g_p's. To check the efficiency of the h_q expansion, we have expanded the first four bound states of the W-He Morse potential in terms of the h_q's. We have found that 14 h_q's reproduce these four wave functions very well, with $\lesssim$ 1% relative error in wave amplitudes.

Based on these preliminary arguments, we now consider the following variational wave functions for the eigenstates of H_{s+a}:

$$\psi(x_s,x_a) = \psi_{asym}\, \Phi(x_a) + \sum_{i=0}^{2} \sum_{j=0}^{N-1} C_{ij}\, \phi_i(x_s) h_j(x_a) \quad , \tag{3.9}$$

where $\Phi(x_a)$ is an error function preventing the He-atom from penetrating into the matter,

$$\Phi(x) = \frac{v}{\sqrt{\pi}} \int_{-\infty}^{x-x_a^0-x_s^0-\sqrt{2}/v} dt\; e^{-v^2t^2} \quad , \tag{3.10}$$

where v is a variational parameter. First consider the bound states $|b\rangle$. Substituting (3.6) with C = 0 and (3.9) into (3.3) and operating

$$\iint dx_s dx_a\; \phi_\ell(x_s) h_m(x_a) \quad ,$$

we obtain a set of coupled algebraic equations for the coefficients C_{ij}'s:

$$\sum_{ij} H_{\ell m,ij} C_{ij}^{b} = \epsilon C_{\ell m}^{b} \quad , \tag{3.11}$$

where

$$H_{\ell m,ij} \equiv \epsilon_i \delta_{\ell i}\delta_{mj} - \delta_{\ell i}P_{mj} + \epsilon_g \bar{U}_{\ell m,ij} \quad , \tag{3.12}$$

and where $\epsilon_i \equiv 2mE_i/\hbar^2$, $\epsilon \equiv 2mE/\hbar^2$, $\epsilon_g \equiv 2\bar{D}m/\hbar^2$, and P_{mj} and $\bar{U}_{\ell m,ij}$, respectively, are given by (B.7) and (B.9). Starting with (3.6) and C = 1, one can obtain a similar equation as (3.11) for the scattering state $|k^+\rangle$. It is noted that unlike the case of bound states, the eigenenergy is already known as $E_k = \hbar^2k^2/2m$. However, there is an additional unknown, S(k), and some additional matrix elements associated with this variable. We have obtained

$$\left[\begin{array}{c|c} H_{\ell m,ij} - \epsilon_k \delta_{\ell i}\delta_{mj} & -H^*_{\ell m} \\ \hline H^*_{ij} & H_{ss} \end{array}\right] \left[\begin{array}{c} C^s_{ij} \\ \hline S(k) \end{array}\right] = \left[\begin{array}{c} -H_{\ell m} \\ \hline H_s \end{array}\right] , \tag{3.13}$$

where $\epsilon_k = k^2$, and $H_{\ell m}$, H_s and H_{ss} are certain integrals involving the error function Φ, (3.10), and are given in Appendix C.

We can now calculate the sticking coefficient $\alpha(k)$ as defined by (2.5). As noted before, our self-trapping model assumes the one-phonon final states $|f\rangle = a^\dagger_q|0\rangle|b\rangle$ and takes as $|k^+\rangle$ the scattering eigenstate of H_{s+a}, and here V_f is H_{int}, (3.2), at $t > 0$. Let

$$-\frac{\hbar^2}{2m} b_\ell^2 \quad , \quad \ell = 1,2,\ldots,\ell_0$$

be the binding energy of the ℓ-th bound state. With the phonon spectrum (3.5), the energy conservation in (2.5) becomes

$$\delta(E_k - E_f) = \frac{1}{\hbar k\sqrt{\bar{D}/M}} \frac{1}{x_s^0\sqrt{2-B_\ell^2}} \{\delta(q-q_0) + \delta(q+q_0)\} \quad , \tag{3.14}$$

where

$$B_\ell = \frac{1}{4\kappa}\sqrt{M/m}\,\sqrt{\hbar^2/m\bar{D}}\,(k^2 + b_\ell^2), \qquad q_0 = \frac{1}{x_s^0}\cos^{-1}(1-B_\ell^2) \quad . \tag{3.15}$$

As for the matrix element in (2.5), from (3.2), (3.6) and (3.9) we have

$$|\langle f|V_f|k^+\rangle|^2 = \frac{(2\kappa\bar{D})^2\hbar}{2N_0M\omega_q}|M_\ell|^2 \tag{3.16}$$

with

$$\begin{aligned} M_\ell &= \sum_{ij} C_{ij}^\ell \int dx\, h_j\phi\{e^{-ikx} - S(k)e^{ikx}\}\int dx\, \phi_i\phi_0\bar{U}'(x)/2\kappa\bar{D} \\ &\quad + \sum_{ij} C_{ij}^\ell \sum_p C_{pj}^s \int dx\, \phi_i\phi_p\, \bar{U}'(x)/2k\bar{D} \\ &= \sum_{ij} C_{ij}^\ell \{Y(j,0) - S(k)Y^*(j,0)\}\frac{N_iN_0}{\kappa K^2}\{KJ(K;i,0;1) - J(K;i,0;2)\} \\ &\quad + \sum_{ij} C_{ij}^\ell \sum_p C_{pj}^s \frac{N_iN_p}{\kappa K^2}\{KJ(K;i,p;1) - J(K;i,p;2)\} \quad , \end{aligned} \tag{3.17}$$

where (A.11) and (C.6) are used. Substituting (3.14) and (3.16) into (2.5) gives

$$\alpha(k) = \frac{8\kappa}{k}\left(\frac{m}{M}\right)^{\frac{1}{2}}\left(\frac{m\bar{D}}{\hbar^2}\right)^{3/2}\sum_{\ell=1}^{\ell_0}\frac{1}{\sqrt{2-B_\ell^2}}\,\frac{1}{k^2 + b_\ell^2}\,|M_\ell|^2 \quad . \tag{3.18}$$

We have numerically solved (3.11) and (3.13) and obtained b_ℓ, C_{ij}^ℓ, S(k) and C_{ij}^s. We have then evaluated $\alpha(k)$ based on (3.15), (3.17) and (3.18). The stability and convergence of the numerical calculation has been checked by changing variational parameters T and v, as well as the number of Gaussian-weighted Hermite polynomials, h_q. To test the validity of our numerical calculations, we have first checked if the numerically obtained binding energies

are reasonable. We have found four bound states with energies -20.087, -9.053, -2.939 and -1.837 in the unit of $Å^{-2}$. Simple estimates of these energies are the four binding energies of the W-He Morse potential, assuming the surface W-atom to be in the ground state ϕ_0. From (A.6), in the same unit of $Å^{-2}$, these estimates are -20.133, -9.530, -2.846 and -0.082, which are close to the numerical results, thus demonstrating the validity of our numerical calculations. Figure 7 contains our final results for T = 2, v = 1 and N = 21. Part a shows that the S-matrix element takes the limit $S(k) \to 1$ as $k \to 0$, demonstrating the dynamical Levinson's theorem, (2.3). Part b shows $\alpha(k)$ as a function of the wave number k. The approximate linear k-dependence of $\alpha(k)$ is seen below $k_c \sim 0.1\ Å^{-1}$. Substituting this into (2.16) with $\kappa = 1.4\ Å^{-1}$ and $\gamma = 48\ Å^{-2}$ gives $\beta \sim 0.6$.

IV. Inverse-Square Potential

In the preceding two sections, we have investigated short-range cases, i.e., the particle-matter interaction potentials decaying faster than x^{-2} at large distance, $x \gg 1$. Due to the existence of the dynamical Levinson's theorem (2.3), we could develop a general and accurate theory for the small-k behavior of the sticking coefficients $\alpha(k)$. As we have found, $\alpha(k) \propto k$, thus verifying that the DWBA is qualitatively correct in this case. One important result is that $\alpha(k) \propto k$ only at $k \lesssim k_c$, and the critical wave number k_c decreases with increasing long-range character of the potentials. In particular, as Fig. 4 shows, the theory predicts that $k_c = 0$ and hence $\alpha(0)$ is finite for an inverse-square potential. In other words, it predicts that the inverse-square potential is a borderline distinguishing between short-range potentials for which $\alpha(0) = 0$ and long-range potentials for which $\alpha(0)$ is finite. In this section, we shall carry out a one-phonon mediated DWBA

calculation of the sticking coefficient for an inverse square potential, and show that this is indeed the case.

Before getting into details, it is useful to look at the problem of sticking coefficients from the viewpoint of formal perturbation theory. The exact scattering eigenstate $|k^+\rangle$ in (2.5) can be written as

$$|k^+\rangle = \sum_{n=0}^{\infty} (G_0 V_f)^n |k\rangle \quad , \tag{4.1}$$

where V_f is a dynamical interaction between the adatom and matter, $|k\rangle$ is an exact scattering eigenstate for a static adatom-matter potential, and $G_0 \equiv (E_k - H + i0^+)^{-1}$ is an adatom propagator with the Hamiltonian H describing the adatom moving in the static adatom-matter potential. Substituting (4.1) into (2.5) provides a power series expansion of $\alpha(k)$ with respect to V_f, whose lowest order, $O(V_f^2)$, is the DWBA. In the case of short-range potentials, the DWBA gives a vanishing $\alpha(0)$, and it has been a challenging question if the inclusion of higher-order terms can bring about a qualitatively different answer, namely a finite $\alpha(0)$. In the case of the inverse-square potential, on the other hand, as we shall see below, the DWBA already gives a finite $\alpha(0)$. Now an important point is that the DWBA is the only term to $O(V_f^2)$. This means that an exact $\alpha(0)$ is also finite in general. In other words, as far as the qualitative small-k-behavior of $\alpha(k)$ is concerned, there is no significant many-body effects in the case of the inverse-square potential.

Another important remark is on the dimensionality of the problem. As we have noted in Section I, a 1-d model of infinite size is physically meaningless for the study of adsorption. Therefore, when one uses the 1-d model, the system size must be finite, so that the phonon spectrum has a gap. In the case of short-range potentials, the number of bound states if finite, and therefore a

cutoff is effectively introduced in the phonon spectrum. This is why the commonly used infinite 1-d model does not show any difficulty. For the inverse-square potential, on the other hand, as we shall see below, there are infinitely many shallow bound states which strongly couple to very "soft" phonons, leading to an infrared catastrophe to be explained. We thus encounter a finite-size problem in a 1-d model for the inverse-square potential. To avoid this problem, we shall extend the commonly used 1-d model to higher dimensions -- two and three -- thereby expecting that the phonon density of states at higher dimensions would suppress the contribution of very soft phonons and remove the infrared catastrophe.

Let us consider a particle of mass m striking the material surface in the normal direction. The Hamiltonian is written in general as

$$H = p^2/2m + H_{ph} + \sum_{i=1}^{N_0} V(\vec{r}-\vec{R}_i) \ . \tag{4.2}$$

Writing $\vec{R}_i = \vec{R}_{i0} + \delta\vec{R}_i$ and following the standard procedures, we divide the third term into a static potential

$$v(z) = \sum_i V(\vec{r}-\vec{R}_{i0}) \tag{4.3}$$

and a dynamical interaction

$$\begin{aligned} V_f &= -\sum_i \vec{\nabla} V(\vec{r}-\vec{R}_{i0})\cdot\delta\vec{R}_i \\ &= -\sum_{\vec{q}\lambda}\sum_{\vec{G}} iN_0(\vec{q}+\vec{G})\cdot\vec{\varepsilon}_{\vec{q}\lambda}\, e^{i(\vec{q}+\vec{G})\cdot\vec{r}} \\ &\quad \times V_{\vec{q}+\vec{G}}\sqrt{\frac{\hbar}{2N_0 M\omega_{\vec{q}\lambda}}}\,(a^{\dagger}_{\vec{q}\lambda} + a_{-\vec{q}\lambda}) \ . \end{aligned} \tag{4.4}$$

In (4.3), we have assumed a translational symmetry parallel to the surface. In (4.4), $\vec{\varepsilon}_{\vec{q}\lambda}$ is a phonon polarization, $V_{\vec{Q}}$ is a Fourier $\vec{Q}$-component, and $\vec{G}$ is a reciprocal lattice vector. Now the one-phonon mediated DWBA for a sticking coefficient $\alpha(k)$ means that in (2.5), the final state is $|f\rangle = a^{\dagger}_{\vec{q}\lambda}|0\rangle|b\rangle e^{i\vec{k}_{\parallel}\cdot\vec{r}_{\parallel}}$, and $|k^{+}\rangle$ and $|b\rangle$ are, respectively, scattering and bound eigenstates of the static potential $v(z)$. Here the subscript $\parallel$ denotes a component parallel to the surface. From (2.5) and (4.4) we have

$$\alpha(k) = \frac{2\pi m}{\hbar^2 k} \sum_{b,\vec{q}\lambda} \delta\{\frac{\hbar^2}{2m}(k^2 - q_{\parallel}^2 + b^2) - \hbar\omega_{\vec{q}\lambda}\} |M|^2 \tag{4.5}$$

with

$$M = \sqrt{\frac{\hbar}{2N_0 M\omega_{\vec{q}\lambda}}}\, iN_0 \sum_{\vec{G} = (0,0,G_z)} \langle b|e^{i(q_z + G_z)z}|k^{+}\rangle$$

$$\times (\vec{q} + \vec{G})\cdot\vec{\varepsilon}_{\vec{q}\lambda} V_{\vec{q}+\vec{G}} \quad . \tag{4.6}$$

In deriving (4.5) and (4.6), we have put $G_{\parallel} = 0$ because at low energy a nonzero $G_{\parallel}$ does not satisfy energy conservation. Moreover, in a standard situation, such as a He-atom colliding on W-matter, we see from energy conservation that $q \ll 1$, which enables us to neglect the $q_{\parallel}^2$-term compared with $\omega_{\vec{q}\lambda}$ in (4.5), and approximate (4.6) as

$$M = \sqrt{\frac{\hbar}{2N_0 M\omega_{\vec{q}\lambda}}}\, N_0 \langle b| \sum_{G_z} e^{iG_z z}\, iG_z \varepsilon^{z}_{\vec{q}\lambda}\, V_{G_z} |k^{+}\rangle \quad . \tag{4.7}$$

We note that the $G_z = 0$ term in (4.6) is negligibly small. On the other hand, one can easily show that

$$v(z) = N_0 \sum_{G_z} e^{iG_z Z} V_{G_z} \quad . \tag{4.8}$$

With (4.8), (4.7) can be written as

$$M = \langle b| \epsilon^z_{\vec{q}\lambda} \sqrt{\frac{\hbar}{2N_0 M\omega_{\vec{q}\lambda}}} \frac{dv(z)}{dz} |k^+\rangle \quad . \tag{4.9}$$

Here it is noteworthy that the result (4.9) justifies replacing the dynamical interaction (4.4) by an effective one,

$$V_f = \sum_{\vec{q}\lambda} \sqrt{\frac{\hbar}{2N_0 M\omega_{\vec{q}\lambda}}} (a^\dagger_{\vec{q}\lambda} + a_{-\vec{q}\lambda}) \frac{dv(z)}{dz} \quad , \tag{4.10}$$

which is a natural extension of the commonly used 1-d model of low-temperature adsorption to higher dimensions.

To explicitly evaluate (4.5) and (4.9) for $\alpha(k)$, we must specify the static potential $v(z)$ and the phonon dispersion $\omega_{\vec{q}\lambda}$. For the static potential we take the form

$$v(z) = \begin{cases} -\frac{\hbar^2}{2m} \gamma z^{-2} & z \geq z_0 \\ \infty & z < z_0 \end{cases} \quad , \tag{4.11}$$

where $z = z_0$ denotes the surface. It is noted that our phonon argument above is not consistent with the long-range potential, (4.11). Conduction electrons will be more relevant than phonons for the long-range interaction.[17] However, as will become clear below, the specific form of the interaction term V_f is not essential for finiteness of $\alpha(0)$, and (4.10) is good enough to study qualitative aspects of quantum adsorption for the long-range potential. For a similar reason, we consider W and He as an example of matter and atom. Clearly the W-He interaction is not of the type (4.11), and the choice of W and He here is simply

for the purpose of specifying the atom and the phonon dispersion. We replace $\omega_{\vec{q}\lambda}$ by ω_q of (3.5), which upon substitution of (3.4) becomes

$$\omega_q = 2\kappa[\frac{\tilde{D}}{M}\{1 - \cos(qx_s^0)\}]^{1/2} \quad . \tag{4.12}$$

This is based on the observation that (4.12) gives a sound velocity ~ 4×10^3 m/s, which is close to the geometrical mean of the longitudinal and transverse sound velocities in three dimensions, ~ $3.4 \sim 10^3$ m/s. With this simplification and

$$\sum_\lambda (\epsilon^z_{\vec{q}\lambda})^2 = 1 \quad , \tag{4.13}$$

the dimensionality, D, appears only in the phonon density of states

$$\Sigma_{\vec{q}} = \frac{L^D}{2\pi(x_s^0)^{D-1}} \int_0^\infty dq\ \rho_D(q) \tag{4.14a}$$

with

$$\rho_D(q) = 2 \quad (D = 1),\ x_s^0 q \quad (D = 2) \text{ and } (x_s^0 q)^2/\pi \quad (D = 3) \quad . \tag{4.14b}$$

Our final task towards the calculation of $\alpha(k)$ is to solve the Schrödinger equation[22]

$$\{-\frac{\hbar^2}{2m}\frac{d^2}{dz^2} + v(z)\}\ \psi = \frac{\hbar^2}{2m}\epsilon^2\psi \quad , \tag{4.15}$$

which is carried out in Appendix D. Figure 8 contains the long-range potential (4.11) in the unit of Å^{-2} with $z_0 = 0.5$ Å and $\mu = \sqrt{\gamma - \frac{1}{4}} = 5.0$, and its bound states calculated from (D.9). From (3.14), (4.5), (4.9) and (4.11)-(4.14), we have

$$\alpha(k) = \frac{(2\gamma)^2 \hbar}{4k\kappa\sqrt{\tilde{D}M}} \sum_{\ell=1}^{\infty} \rho_D(q_0) \frac{1}{\sqrt{2 - B_\ell^2}} \frac{1}{k^2 + b_\ell^2} |\langle \ell | z^{-3} | k^+ \rangle|^2 \quad , \tag{4.16}$$

where b_ℓ is the ℓ-th b as given by (D.9), and $|\ell\rangle$ is the ℓ-th bound state (D.14), with the first bound state being the lowest bound state. Substituting (D.4), (D.6), (D.14) and (D.18) into (4.16) gives

$$\alpha(k) = \frac{4\pi\hbar}{\kappa\sqrt{\tilde{D}M}} \frac{\gamma^2}{z_0^2} e^{-\pi\mu} |J_\nu(kz_0)|^{-2} \sum_{\ell=1}^{\infty} \rho_D(q_0)$$

$$\times \frac{1}{\sqrt{2 - B_\ell^2}} \frac{1}{k^2 + b_\ell^2} |I_{-\nu+1}(b_\ell z_0) - I_{\nu-1}(b_\ell z_0)|^{-2} |M_\ell|^2 \tag{4.17}$$

where $\nu = \sqrt{\frac{1}{4} - \gamma^2}$ and

$$M_\ell \equiv \int_{z_0}^{\infty} dz\, z^{-3} \{J_\nu(kz) J_{-\nu}(kz_0) - J_{-\nu}(kz) J_\nu(kz_0)\}$$

$$\times \{I_\nu(b_\ell z) - I_{-\nu}(b_\ell z)\} \quad . \tag{4.18}$$

For given values of parameters z_0, μ and k, one can calculate the prefactor in (4.17) and bound-state spectrum b_ℓ by (D.9), (D.11) and (D.12), which in turn determines B_ℓ and $\rho_D(q_0)$ by (3.15) and (4.14b), and $|I_{-\nu+1}(b_\ell z_0) - I_{\nu-1}(b_\ell z_0)|^{-2}$ by (D.11). Finally, the matrix element (4.18) can be evaluated numerically, with some remarks given in Appendix E.

We can now discuss some properties of $\alpha(k)$. First of all, the finiteness of $\alpha(0)$ can be seen as follows. Consider the lowest bound-state contribution in (4.16). It is clear in this expression that in the limit $k \to 0$, the k-dependence of $\alpha(k)$ is determined by that of the quantity $|k^+\rangle^2/k$, which, however, approaches a constant due to the $\sqrt{k}$-dependence of $|k^+\rangle$ in the limit $k \to 0$, (D.7). Therefore, the lowest-bound-state contribution to $\alpha(0)$ and hence the

value of $\alpha(0)$ itself is constant. An important point here is that this conclusion of finite $\alpha(0)$ does not use details of the interaction H_{int}. Thus, we have seen that the finiteness of $\alpha(0)$ is a general consequence of the inverse-square potential. Secondly, we have observed a logarithmic divergence of $\alpha(k)$ in the 1-d case,

$$\alpha(k)_{D=1} \propto - \ln k \quad \text{for } k \to 0 \ . \tag{4.19}$$

To see the origin of this catastrophe, consider the matrix element M_ℓ in the limit $k,b \to 0$. In this limit, substituting (D.2) and (D.11) into (4.18) gives

$$M_\ell \propto \int_1^\infty dz\ z^{-2}(z^\nu - z^{-\nu})\{\frac{\Gamma(1-\nu)}{\Gamma(1+\nu)}(\delta_\ell z)^\nu - (\delta_\ell z)^{-\nu}\}$$

$$\propto \frac{\Gamma(1-\nu)}{\Gamma(1+\nu)}\,\delta_\ell^\nu\,\frac{1}{1-2\nu} - \delta_\ell^{-\nu}\,\frac{1}{1+2\nu} \ , \tag{4.20}$$

where $\delta_\ell \equiv b_\ell z_0/2$. From (4.20) and (D.12) we have

$$|M_\ell|^2 \propto - \nu^2/|1+2\nu|^4 = \text{constant}. \tag{4.21}$$

On the other hand, in the same limit $k,b \to 0$, (D.2), (3.15), (D.18) and (D.19) give

$$|J_\nu(kz_0)|^2 \to \text{constant}, \quad B_\ell \to 0$$

$$|I_{-\nu+1}(\delta_\ell) - I_{\nu-1}(\delta_\ell)| \propto \delta_\ell^{-1} \ . \tag{4.22}$$

Substituting (4.21) and (4.22) into (4.17) and using the density of bound states (D.13), we find the contribution of the bound states $0 \le b \le b_0 \ll 1$ to $\alpha(k)$ as

$$\propto \int_0^{b_0} db\ \rho_D(k^2 + b^2)\,\frac{b}{k^2 + b^2} \tag{4.23}$$

which, for D = 1, diverges logarithmically in the limit $k \to 0$. That is, in the limit $k \to 0$, each of the contributions from very shallow bound states remains finite, and $\alpha(k)$ diverges logarithmically due to the linearly diverging density of bound states. However, as we have pointed out in Section I, the obtained infrared catastrophe does not imply a new surface many-body problem, but reveals a pathological aspect of the infinite 1-d model.

Finally, we have numerically evaluated (4.17) and (4.18) for the D = 1, 2 and 3 cases. Figure 9 contains sticking coefficients $\alpha(k)$ as functions of the wave number k. The parameters used are $z_0 = 0.5$ Å and $\mu = 5.0$. Note that a logarithmic divergence of $\alpha(k)$ in the D = 1 case is spurious. Although the infinite 2-d model has in general the same pathological aspect as the 1-d model in that there can be no lattice formations in one and two dimensions just as there can be no spontaneous magnetizations in the isotropic Heisenberg model in these dimensions,[20] the spurious contribution of very soft phonons is suppressed by the decreasing phonon density of states at $q \to 0$ [cf. (4.14b)], as a tiny difference between $\alpha(0)$ and $\alpha(2)$ in the D = 2 curve demonstrates. The results for the cases D = 2 and 3 demonstrate finite $\alpha(0)$ for the inverse-square potential.

V. Summary

In this paper we have developed a new theory of quantum sticking coefficients at 0 K. Based on the dynamical Levinson's theorem, we have first considered the cases where the adatom-matter interaction potentials decay faster than x^{-2}. We have demonstrated that the many-body motion of adatom-matter system is not essential in determining the low-energy behavior of the sticking coefficients. The essence is instead in the long-distant part of the interaction. The theory predicts that $\alpha(k) \propto k$ at $k \leq k_c$, and that the critical

wave number k_c decrease with increasing long-range character of the adatom-matter interaction. To give a quantitative measure of k_c, we have introduced the standard number β in analogy to the "standard value" in the Lindeman melting formula. To determine β, we have considered a self-trapping model for the W-He system. By carrying out precise numerical evaluations of $\alpha(k)$, we have determined that $\beta \sim 0.6$. As a test of the present theory, we have then applied our results to the case of ^{4}He-atom colliding with a liquid ^{4}He surface, for which accurate experimental data are available. The theory predicts that $\alpha(k) \propto k$ at $k \lesssim 0.01$ Å^{-1}, in good agreement with experiments. Next, we have considered the inverse-square potential. Our study based on the dynamical Levinson's theorem has already verified that $k_c \to 0$ as the potential approaches the inverse-square one, which strongly indicates a finite $\alpha(0)$ for the inverse-square potential. We have carried out the one-phonon-mediated DWBA for the quantum sticking coefficient at 0 K and have shown that the inverse-square potential is a borderline distinguishing between "short-range" potentials for which $\alpha(0) = 0$ and long-range potentials for which $\alpha(0) \neq 0$. We note that the finite $\alpha(0)$ result of DWBA would hardly be changed qualitatively by including higher-order corrections. It is also noted that this result depends on the fact that the scattering wave function has a $\sqrt{k}$-singularity in the small-k limit, in sharp contrast to the linear k-dependence in the case of short-range potentials, and therefore it is a general consequence of the inverse-square potential. In brief, the essence of quantum sticking coefficients at 0 K is in the k-dependence of the scattering wave function $|k^+\rangle$ in the low-energy limit $k \to 0$. For short-range potentials, $|k^+$ has a linear k-dependence which leads to a linearly vanishing $\alpha(k)$. On the other hand, for long-range potentials, $|k^+\rangle$ has a $\sqrt{k}$-singularity leading to a finite $\alpha(0)$.

Acknowledgments

This research was supported by the Air Force Office of Scientific Research (AFSC), United States Air Force, under Contract F49620-86-C-0009, the Office of Naval Research and the National Science Foundation under Grant CHE-8620274. The United States Government is authorized to reproduce and distribute reprints notwithstanding any copyright notation hereon.

Appendix A. Some Results about Morse Potentials

The one-body problem for a Morse potential,

$$\{-\frac{\hbar^2}{2m}\frac{d^2}{dx^2} + D(e^{-\kappa x} - 2e^{-\kappa x})\}\,\phi(x) = E\phi(x) \quad , \tag{A.1}$$

is exactly solvable.[14] The bound states are

$$\phi_n = N_n e^{-z/2}\, z^{(K-2n-1)/2}\, F_n(z) \quad , \tag{A.2}$$

where

$$K \equiv 2\sqrt{2mD}/\hbar\kappa \quad , \quad z \equiv Ke^{-\kappa x} \quad , \tag{A.3}$$

and the F_n's are Laguerre polynomials,

$$F_n(z) = L_n^{K-2n-1}(z) \equiv \sum_{m=0}^{n}(-1)^m\binom{K-n-1}{n-m}\frac{z^m}{m!} \tag{A.4}$$

satisfying the differential equation

$$z\frac{d^2F}{dz^2} + (K-2n-z)\frac{dF}{dZ} + nF = 0 \quad . \tag{A.5}$$

The corresponding binding energies are

$$E_n = -\frac{\kappa^2\hbar^2}{8m}(K-2n-1)^2 \qquad 0 \le n \le [(K-1)/2] \quad . \tag{A.6}$$

The normalization constant N_n is determined by the orthonormal condition

$$\delta_{ij} = \int_{-\infty}^{\infty} dx\, \phi_i(x)\phi_j(x)$$

$$= \frac{N_iN_j}{\kappa}\int_0^{\infty} dz\, e^{-z}z^{K-i-j-2}\, L_i^{K-2i-1}(z)\, L_j^{K-2j-1}(z) \quad . \tag{A.7}$$

The integral in (A.7) is a special case ($\xi = 0$) of the Nieto and Simmons

integral[16]

$$J(K;i,j;\xi) \equiv \int_0^\infty dz\, e^{-z} z^{K-i-j-2+\xi} L_i^{K-2i-1}(z)\, L_i^{K-2j-1}(z)$$

$$= \sum_{m=0}^{j} (-1)^m \binom{K-j-1}{j-m} \frac{1}{m!} \frac{\Gamma(K-i-j-1+\xi+m)\Gamma(j+1-\xi-m)}{i!\Gamma(j-i+1-\xi-m)} \quad , \tag{A.8}$$

where Γ is a gamma function. In particular,

$$J(K;i,i;0) = \binom{K-i-1}{i} \Gamma(K-2i-1) \quad , \tag{A.9}$$

from which the normalization constant N_i is determined as

$$N_i = \sqrt{Ki!(K-2i-1)/(k-i-1)!} \quad . \tag{A.10}$$

Similarly,

$$\int_{-\infty}^{\infty} dx\, \phi_i \phi_j e^{\ell\kappa x} = \frac{K^\ell N_i N_j}{\kappa} J(K;i,j;-\ell) \quad . \tag{A.11}$$

Appendix B. Hermite Polynomials and Related Integrals

The Hermite polynomials

$$H_n(x) = \sum_{r=0}^{[n/2]} (-1)^r (2r-1)!! \binom{n}{2r} x^{n-2r} \tag{B.1}$$

have the properties

$$H_n'' - xH_n' + nH_n = 0 \tag{B.2}$$

$$H_{n+1} - xH_n + nH_{n-1} = 0 \tag{B.3}$$

$$H_n' = nH_{n-1} \tag{B.4}$$

$$\int_{-\infty}^{\infty} dx\, e^{-x^2/2} H_m H_n = \sqrt{2\pi}\, n!\, \delta_{mn} \quad . \tag{B.5}$$

Using (B.2)-(B.4), we obtain

$$h_n'' = \tilde{N}_n e^{-T^2x^2/4}\, T^2(T^2x^2/4 - 1/2 - n)H_n(Tx) \quad . \tag{B.6}$$

With (B.3), (B.5) and (B.6) we have

$$\begin{aligned} P_{mn} &\equiv \int_{-\infty}^{\infty} dx\, h_m h_n'' \\ &= \tilde{N}_m \tilde{N}_n\, T \int_{-\infty}^{\infty} dx\, e^{-x^2/2}\, (x^2/4 - 1/2 - n)H_m H_n \\ &= \frac{T^2}{4}[-(2n+1)\,\delta_{mn} + \sqrt{(n+1)(n+2)}\,\delta_{m-1,n+1} \\ &\quad + \sqrt{n(n-1)}\,\delta_{m+1,n-1}] \quad . \end{aligned} \tag{B.7}$$

Next, using the expansion (B.1) we have

$$\begin{aligned} Q_{mn}(A) &\equiv \int_{-\infty}^{\infty} dx\, h_m e^{-Ax}\, h_n \\ &= \frac{\tilde{N}_m \tilde{N}_n}{T} \sum_{r=0}^{[m/2]} \sum_{r'=0}^{[n/2]} (-1)^{r+r'}(2r-1)!!\,(2r'-1)!! \\ &\quad \times \binom{m}{2r}\binom{n}{2r'} \int_{-\infty}^{\infty} dx\, e^{-x^2/2 - Ax/T}\, x^{m-2r+n-2r'} \\ &= \frac{(-A/T)^{m+n}}{\sqrt{m!n!}}\, e^{A^2/2T^2} \sum_{r=0}^{[m/2]} \sum_{r'=0}^{[n/2]} \sum_{k=0}^{[(m+n)/2]-r-r'} (-1)^{r+r'} \\ &\quad \times (2r-1)!!\,(2r'-1)!!\,(2k-1)!!\,(A/T)^{-2r-2r'-2k} \\ &\quad \times \binom{m}{2r}\binom{n}{2r'}\binom{m+n-2r-2r'}{2k} \quad . \end{aligned} \tag{B.8}$$

Using (A.11) and (B.8) we evaluate the integral

$$\bar{U}_{\ell m,ij} \equiv \frac{1}{D}\iint dx_s\, dx_a\, \phi_\ell(x_s)\,\phi_i(x_s)\bar{U}(x_a-x_s)\,h_m(x_a)h_j(x_a)$$

$$= \int dx\, \phi_\ell\phi_i e^{2\kappa x}\int dx\, h_m\, h_j\, e^{-2\kappa x} - 2\{2\kappa \to \kappa \text{ in the first term}\}$$

$$= \frac{K^2 N_\ell N_i}{\kappa}\, J(K;\ell,i;-2)\, Q_{mj}(2\kappa)$$

$$- 2\frac{KN_\ell N_i}{\kappa}\, J(K;\ell,i;-1)\, Q_{mj}(\kappa) \quad . \tag{B.9}$$

Appendix C. Some Integrals Involving Φ

First consider the integral

$$H_{\ell m} \equiv \frac{2m}{\hbar^2}\iint dx_s\, dx_a\, \phi_\ell\phi_0\, h_m\, e^{-ikx_a}$$

$$\times \{-\frac{\hbar^2}{2m}(-2ik\phi' + \phi'') + \bar{U}(x_a-x_s)\phi\}$$

$$\equiv -\delta_{\ell 0}A + \varepsilon_g B \quad . \tag{C.1}$$

With (3.8), (3.10) and (B.3), A becomes

$$A = (-2ikv/\sqrt{\pi} + 2\sqrt{2}v^2/\sqrt{\pi})R(m,ik)$$

$$- \frac{2v^3}{\sqrt{\pi}T}\{\sqrt{m+1}R(m+1,ik) + \sqrt{m}R(m-1,ik)\} \quad , \tag{C.2}$$

where we have defined

$$R(m,c) \equiv \int dx\, h_m e^{-cx} e^{-v^2(x-\sqrt{2}/v)^2} \quad . \tag{C.3}$$

Using (3.8) and (B.1) and carrying out a standard Gaussian integral, we obtain

$$R(m,c) = \sqrt{\sqrt{2\pi}/m!T}\; e^{-2}e^{(2\sqrt{2}u-c)^2/(T^2+4v^2)}$$

$$\times \sum_{r=0}^{[m/2]} \sum_{\ell=0}^{[m/2]-r} (-1)^r (2r-1)!! \; (2\ell-1)!! \; \binom{m}{2r} \binom{m-2r}{2\ell}$$

$$\times \left(\frac{2T^2}{T^2+4v^2}\right)^{m-2r-\ell+1/2} \left(\frac{2\sqrt{2}v-c}{T}\right)^{m-2r-2\ell} \quad . \tag{C.4}$$

As for the term B, from (3.4) and (A.11) it becomes

$$B = \frac{K^2 N_\ell N_0}{\kappa} J(K;\ell,0;-2)\; Y(m,2\kappa) - 2\frac{KN_\ell N_0}{\kappa} J(K;\ell,0;-1)\; Y(m,\kappa) \quad , \tag{C.5}$$

where we have defined

$$Y(m,c) \equiv \int dx\; h_m \Phi\; e^{-(c+ik)x} \quad . \tag{C.6}$$

Integrating by parts and using (3.8), (3.10), (B.3), and (B.4), we have

$$Y(m,c) = \frac{1}{c+ik} \frac{v}{\sqrt{\pi}} \int dx\; h_m\; e^{-(c+ik)x}\; e^{-v^2(x-\sqrt{2}/v)^2}$$

$$+ \frac{1}{c+ik} \frac{T}{2}\{\sqrt{m}\; Y(m-1,c) - \sqrt{m+1}\; Y(m+1,c)\} \quad . \tag{C.7}$$

From (C.3) and (C.7) we have the recursion relation

$$Y(m+1,c) = -\frac{2(c+ik)}{T\sqrt{m+1}}\; Y(m,c) + \sqrt{\frac{m}{m+1}}\; Y(m-1,c)$$

$$+ \frac{2v}{T\sqrt{\pi}\sqrt{m+1}}\; R(m,c+ik) \quad . \tag{C.8}$$

The first term Y(0,c) cannot be evaluated analytically, but the dimension of integrations can be reduced from 2 to 1. In the expression

$$W(c,T,k,v) \equiv Y(0,c) = \int dx\; h_0 \Phi\; e^{-(c+ik)x}$$

$$= \frac{N_0 v}{\sqrt{\pi}} \int_{-\infty}^{\infty} dx\; e^{\frac{-T^2}{4}(x+\sqrt{2}/u)^2 - (c+ik)(x+\sqrt{2}/u)} \int_{-\infty}^{x} dt\; e^{-v^2 t^2} \quad , \tag{C.9}$$

we make the variable change $t \to x+t$, and the order of integrations as

$$\int_{-\infty}^{\infty} dx \int_{-\infty}^{x} dt \to \int_{-\infty}^{\infty} dx \int_{-\infty}^{0} dt \to \int_{-\infty}^{0} dt \int_{-\infty}^{\infty} dx \quad .$$

Carrying out a Gaussian integral over x, we reach the results

$$Y(0,c) = \frac{2\bar{N}_0 v}{\sqrt{4v^2 + T^2}} e^{-2} e^{(c+ik-2\sqrt{2}v)^2/(4v^2+T^2)}$$

$$\times \int_{-\infty}^{0} dt \exp\left[- \frac{v^2T^2}{4v^2+T^2} \{t^2 - \frac{4}{T^2}(T^2/\sqrt{2}v + c + ik)t\}\right] \quad . \qquad (C.10)$$

Next consider integrals which involve the error function Φ twice. First consider

$$H_{ss}^1(k) \equiv - \frac{2m}{\hbar^2} \iint dx_s \, dx_a \, \phi_0^2 \, \Phi^2 \, e^{2ikx_a} \, \bar{U}(x_a - x_s)$$

$$= - \frac{\epsilon_g K^2 N_0^2}{\kappa} J(K;0,0;-2) \, G(k,2\kappa) + \frac{2\epsilon_g K N_0^2}{\kappa} J(K;0,0;-1) G(k,\kappa) \quad , \qquad (C.11)$$

where

$$G(k,c) \equiv \int dx \, \Phi^2 \, e^{(2ik-c)x} \quad . \qquad (C.12)$$

With the use of (3.10), an integration by parts and (C.9), we have

$$G(k,c) = \frac{e^{-2}}{c-2ik} \sqrt{\frac{4u}{\sqrt{2\pi}}} \, W(c-2\sqrt{2}v, 2v, -2k, v) \quad . \qquad (C.13)$$

We must also carry out the following integrations:

$$H_s^2 \equiv \int dx \, \Phi(\Phi'' - 2ik\Phi') = - (ik + v/\sqrt{2\pi}) \quad . \qquad (C.14)$$

$$H_{ss}^2 \equiv \int dx \, \Phi \, (\Phi'' + 2ik\Phi') \, e^{2ikx} = - \frac{v}{\sqrt{2\pi}} e^{-k^2/2v^2} + 2\sqrt{2}ik/v \quad . \qquad (C.15)$$

H_s and H_{ss} in (3.13) are then given by

$$H_s = H_{ss}^1(0) + H_s^2 \quad . \qquad (C.16)$$

$$H_{ss} = H^1_{ss}(k) + H^2_{ss} \quad . \tag{C.17}$$

Appendix D. Solution of (4.15)

The solution of (4.15) can be written as

$$\psi = \sqrt{z}\,[AJ_\nu(\varepsilon z) + BJ_{-\nu}(\varepsilon z)] \quad , \tag{D.1}$$

where $\gamma \equiv 1/4 - \nu^2 \equiv 1/4 + \mu^2$, and A and B are constants of integration. J_ν is the Bessel function of the first kind,[18]

$$J_\nu(z) = (z/2)^\nu \sum_{n=0}^{\infty} \frac{(-1)^n (z/2)^{2n}}{n!\Gamma(\nu + n + 1)} \quad . \tag{D.2}$$

Since (4.15) is real, we can take ψ as real. First consider a scattering state, where $\varepsilon = k$ is positive. Noting that $J^*_\nu(z) = J_{-\nu}(z)$, we can satisfy the reality condition and the boundary condition $\psi(z_0) = 0$ by taking

$$B^* = A = iJ_{-\nu}(kz_0) \quad . \tag{D.3}$$

With (D.1) and (D.3) we now write the scattering state as

$$|k^+\rangle = iN_k\sqrt{z}[J_\nu(kz)J_{-\nu}(kz_0) - J_{-\nu}(kz)J_\nu(kz_0)] \quad . \tag{D.4}$$

To find the normalization factor N_k, note the asymptotic property at $|z| \to \infty$,[18]

$$J_\nu(z) \sim \sqrt{\frac{2}{\pi z}} \cos\left(z - \frac{2\nu + 1}{4}\pi\right) \quad . \tag{D.5}$$

By setting the prefactor of the e^{-ikz} component in $|k^+\rangle$ at $z \to \infty$ equal to 1, N_k is given by

$$\begin{aligned} N_k &= \sqrt{2\pi k}\,\left|J_{-\nu}(kz_0)\, e^{-\pi\mu/2} - J_\nu(kz_0)\, e^{\pi\mu/2}\right|^{-1} \\ &\simeq \sqrt{2\pi k}\, e^{-\pi\mu/2}/|J_\nu(kz_0)| \quad , \end{aligned} \tag{D.6}$$

where in the second expression we have assumed $\mu \gg 1$. The case $\mu \lesssim 1$ corresponds to an unrealistically narrow and deep potential. A particular interest is in the limit $k \to 0$, where from (D.2), (D.4) and (D.6) we have for $z \ll k^{-1}$

$$|k^+\rangle_{k\to 0} = i\sqrt{kz/\mu}\,[z/z_0)^{\nu} - (z/z_0)^{-\nu}] \propto \sqrt{k} \quad . \tag{D.7}$$

This $\sqrt{k}$-singularity of the scattering state $|k^+\rangle$ is in sharp contrast to the linear k-dependence of $|k^+\rangle$ for the short-range potentials, (2.12). As we see in the text, this is the key point of finite $\alpha(0)$ for the inverse-square potential.

Next we consider bound states. In this case, $\varepsilon = ib$ (b = positive). The reality condition is met by taking

$$B = A^* e^{-\pi\mu} \quad . \tag{D.8}$$

On the other hand, the finiteness requirement for the wave function at $z \to \infty$ leads to a pure imaginary A. With (D.8) and the fact that A is pure imaginary, the boundary condition $\psi(z_0) = 0$ provides the quantization of bound states,

$$I_{\nu}(bz_0) - I_{-\nu}(bz_0) = 0 \quad , \tag{D.9}$$

where $I_{\nu}(z)$ is the modified Bessel function of the first kind.[18] Alternatively, one can look at the Jost function f(-k), the prefactor of the e^{-ikz} component in the scattering state $|k^+\rangle$ at $z \to \infty$,

$$f(-k) = J_{\nu}(kz_0)\, e^{\pi\mu/2} - J_{-\nu}(kz_0)\, e^{-\pi\mu/2} \quad , \tag{D.10}$$

whose zeroes at $k = ib$ in the complex k-plane describe the bound states. The condition $f(-ib) = 0$ is nothing but (D.9). Unlike the short-range potentials studied in Section II, the inverse-square potential has an infinite number of

bound states. To see this, consider the limit $bz_0 \to 0$. In this limit, only the $n = 0$ term in the power series expansion of $I_\nu(z)$,[18]

$$I_\nu(z) = (z/2)^\nu \sum_{n=0}^{\infty} \frac{(z/2)^{2n}}{n!\Gamma(\nu + n + 1)} \quad , \tag{D.11}$$

is kept and the quantization condition (D.9) becomes

$$b = \frac{2}{z_0} e^{\frac{1}{2\nu} \ln\frac{\Gamma(1+\nu)}{\Gamma(1-\nu)}} e^{-\frac{\pi n}{\mu}} \quad , \tag{D.12}$$

where n is any integer such that $bz_0 \ll 1$. That is, there are infinitely-many shallow bound-states, whose density of states diverges at $b \to 0$ as

$$\rho(b) = \mu/\pi b \quad . \tag{D.13}$$

Finally, to normalize the bound states, we use (D.8) and $\mathrm{Re}A = 0$ to write

$$|b\rangle = iN_b\sqrt{z}\,[I_\nu(bz) - I_{-\nu}(bz)] \equiv iN_b\sqrt{z}\,[-\frac{2\sin(\pi\nu)}{\pi} K_\nu(bz)] \quad . \tag{D.14}$$

With the property[19]

$$\{\frac{z^2}{2}[K_\nu^{\,2}(\zeta z) - K_{\nu-1}(\zeta z)K_{\nu+1}(\zeta z)]\}' = zK_\nu^{\,2}(\zeta z) \quad , \tag{D.15}$$

the normalization integral is carried out to give

$$N_b = \frac{\sqrt{2}}{z_0} \frac{\pi}{2\sinh\mu} [K_{\nu-1}(bz_0)K_{\nu+1}(bz_0)]^{-\frac{1}{2}} \quad . \tag{D.16}$$

It is noted that $k_\nu(bz_0) = 0$ due to (D.9) and (D.14). With the use of (D.14) and the recursion formula[18]

$$I_{\nu-1}(z) - I_{\nu+1}(z) = (2\nu/z)I_\nu(z) \quad , \tag{D.17}$$

(D.16) can be written as

$$N_b = \frac{\sqrt{2}}{z_0}\left|I_{-\nu+1}(bz_0) - I_{\nu-1}(bz_0)\right|^{-1} \quad , \tag{D.18}$$

which is more suitable for numerical calculations based on (D.11). In particular, in the limit $b \to 0$, from (D.11), (D.12) and (D.18), we have

$$N_b \propto b\left|1 - (bz_0/2)^2/\nu(1-\nu)\right|^{-1} \propto b \quad . \tag{D.19}$$

Appendix E. Evaluation of (4.18)

Here we give some technical remarks on the numerical evaluation of (4.18). Using $\bar{k} \equiv kz_0$ and $\bar{b} \equiv bz_0$, one can write (4.18) as

$$M_\ell = \frac{1}{z_0}[J_{-\nu}(\bar{k})O(\bar{b},\bar{k}) + \text{c.c.}] \quad , \tag{E.1}$$

where

$$O(\bar{b},\bar{k}) \equiv \int_1^\infty dz\, z^{-2}[I_\nu(\bar{b}z) - I_{-\nu}(\bar{b}z)]J_\nu(\bar{k}z) \quad . \tag{E.2}$$

The first thing to do is to replace ∞ by a finite z_m in (E.2). For a given $\bar{b}$, z_m is roughly a classical turning point of the potential (4.11),

$$z_m \approx \sqrt{\gamma}/\bar{b} \quad . \tag{E.3}$$

Next we evaluate the Bessel functions $I_\nu = I^*_{-\nu}$ and J_ν for the variable ranges $\bar{b} \le \bar{b}z \le \sqrt{\gamma}$ and $\bar{k} \le \bar{k}z \le \bar{k}z_m$. For a realistic situation $\sqrt{\gamma} \lesssim 10$, the Bessel function I_ν can be evaluated accurately by the power series expansion (D.11). On the other hand, even for an interesting situation, $\bar{k} \sim 1$, $\bar{k}z_m \approx \bar{k}\sqrt{\gamma}/\bar{b}$ can be large for small $\bar{b}$. We have found that the power series expansion (D.2) is good for $z \lesssim 30$. For $z > 30$, one can use Hankel's asymptotic expansion,[18]

$$J_\nu(z) = \sqrt{\frac{2}{\pi z}}[P(\nu,z)\cos(z - \frac{2\nu+1}{4}\pi) - Q(\nu,z)\sin(z - \frac{2\nu+1}{4}\pi)] \quad , \tag{E.4}$$

where with $\xi \equiv 4\nu^2$,

$$P(\nu,z) = 1 - \frac{(\xi-1)(\xi-9)}{2!\,(8z)^2} + \frac{(\xi-1)(\xi-9)(\xi-25)(\xi-49)}{4!\,(8z)^4} \cdots \tag{E.5}$$

$$Q(\nu,z) = \frac{\xi-1}{8z} - \frac{(\xi-1)(\xi-9)(\xi-25)}{3!\,(8z)^3} + \cdots \tag{E.6}$$

Though it is a bit time-consuming, the integral representation[18]

$$I_\nu(z) = \frac{(z/2)^\nu}{\sqrt{\pi}\Gamma(\nu+\frac{1}{2})}\int_0^\pi d\theta\, \cos(z\cos\theta)\, \sin^{2\nu}\theta \tag{E.7}$$

is good for an arbitrary argument z. A caution for the integration in (E.7) is that at small $\theta \ll 1$, the integrand oscillates with a period ~ θ.

References

1) D. Eichenauer and J. P. Toennies, Sonderforschungsbereich 126 Goettingen/Clausthal (Germany, F. R.), pp. 1-14.

2) M. D. Stiles and J. W. Wilkins, Phys. Rev. Lett. 54, 595 (1985).

3) J. E. Lennard-Jones and A. F. Devonshire, Proc. Roy. Soc. London, Sev. A, 156, 6, 36 (1936).

4) B. McCarroll and G. Ehrlich, J. Chem. Phys. 38, 523 (1963).

5) G. Doyen, Phys. Rev. B 22, 497 (1980); Surf. Sci. 117, 85 (1982).

6) T. R. Knowles and H. Suhl, Phys. Rev. Lett. 39, 1417 (1977).

7) F. O. Goodman, J. Chem. Phys. 55, 5742 (1971); N. Garcia and J. Ibanez, J. Chem. Phys. 64, 4803 (1976).

8) D. O. Edwards, Physica 109 & 110B, 1531 (1982). See also M. Sinvani, M. W. Cole and D. L. Goodstein, Phys. Rev. Lett. 51, 188 (1983).

9) L. I. Schiff, Quantum Mechanics (McGraw-Hill, New York, 1968), p. 344.

10) S. G. Chung and T. F. George, J. Math. Phys. 28, 1103 (1987)..

11) E. M. Lifshitz and L. P. Pitaevskii, Landau and Lifshitz Course of Theoretical Physics Vol. 5: Statistical Physics Part 1 (Pergamon Press, New York, 1980), p. 537.

12) T. Y. Wu and T. Ohmura, Quantum Theory of Scattering (Prentice-Hall, Englewood Cliffs, New Jersey, 1962).

13) J. M. Ziman, Principles of the Theory of Solids (Cambridge University Press, Cambridge, 1972), p. 65.

14) P. M. Morse, Phys. Rev. 34, 57 (1929).

15) L. A. Girifalco and V. G. Weizer, Phys. Rev. 114, 687 (1959); F. O. Goodman and J. D. Gillerlain, J. Chem. Phys. 57, 3645 (1972).

16) M. M. Nieto and L. M. Simmons, Jr., Phys. Rev. A 19, 438 (1979).

17) D. Lando and L. J. Slutsky, J. Chem. Phys. 52, 1510 (1970).

18) M. Abramowitz and I. A. Stegun, Handbook of Mathematical Functions (National Bureau of Standards, Applied Mathematics Series 55, 1972), Chap. 9.

19) I. S. Gradshteyn and I. M. Ryzhik, Tables of Integrals, Series and Products (Academic Press, New York, 1980), p. 633.

20) N. W. Ashcroft and N. D. Mermin, Solid State Physics (Holt, Rinehart and Winston, New York, 1976), p. 704.

21) G. Brivio and T. B. Grimley, Surf. Sci. 161, L573 (1985); Phys. Rev. B 35, 5969 (1987).

22) A slightly different x^{-2} potential was analyzed by F. O. Goodman, Surf. Sci. 27, 157 (1971).

Figure Captions

1. (a) Three-dimensional geometry for the scattering eigenstate characterized by the parallel and perpendicular wave numbers, k_x and k_z.

   (b) One-dimensional simplification when the parallel and perpendicular motions are approximately separable.

   (c) Two-dimensional T-shape model for low-temperature adsorption.

2. Static square-well potential.

3. Schematic figure of the reduced potential U(x) and its modifications (dashed lines) in the region $R' < x < R$.

4. k_c as a function of the exponent n for $\gamma = 20$ and $\beta = 0.6$.

5. Self-trapping model for He adsorption on W.

6. One-particle energy spectra for the surface W-atom and He-atom.

7. (a) $|S|$ and ReS vs. k. It is seen that $S \to 1$ as $k \to 0$.

   (b) $\alpha(k)$ vs. k. Below $k_c \sim 0.1$ Å^{-1}, α has an approximate linear dependence on k.

8. The solid curve is the long-range potential (4.11) in the unit of Å^{-2} with $z_0 = 0.5$ Å and $\mu = 5.0$. The horizontal solid lines denote its bound states calculated from (D.9). Bound states with very small energies are described by (D.12).

9. $\alpha(k)$ vs. k for D = 1, 2 and 3. The parameters are $z_0 = 0.5$ Å and $\mu = 5.0$. For the D = 1 case, a spurious logarithmic singularity is seen for small k, as described in the text. The other cases D = 2 and 3 demonstrate finite quantum sticking coefficients at $k \to 0$.

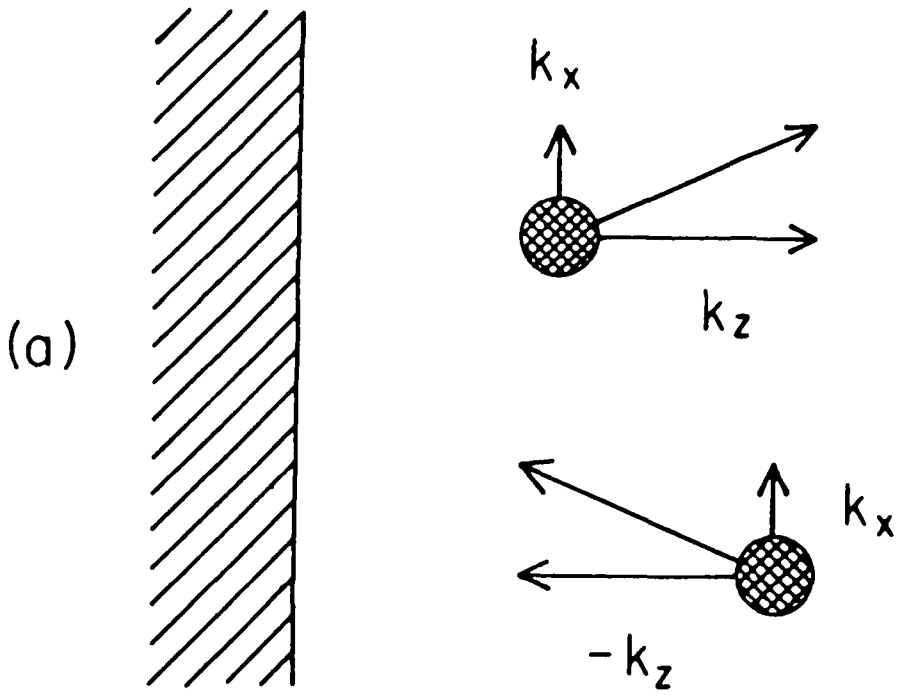

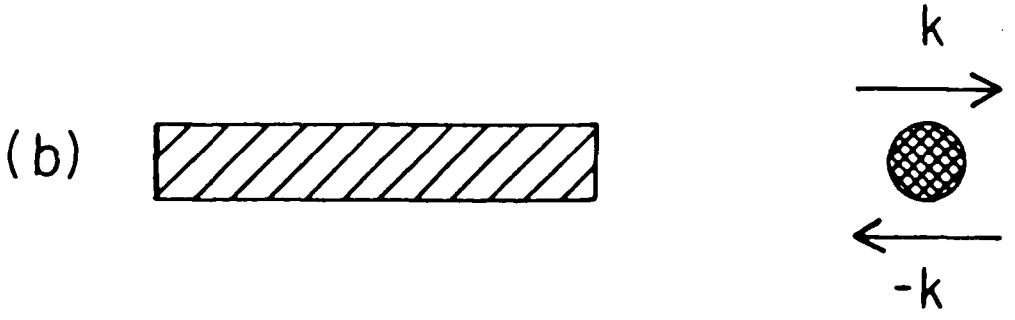

Fig. 1

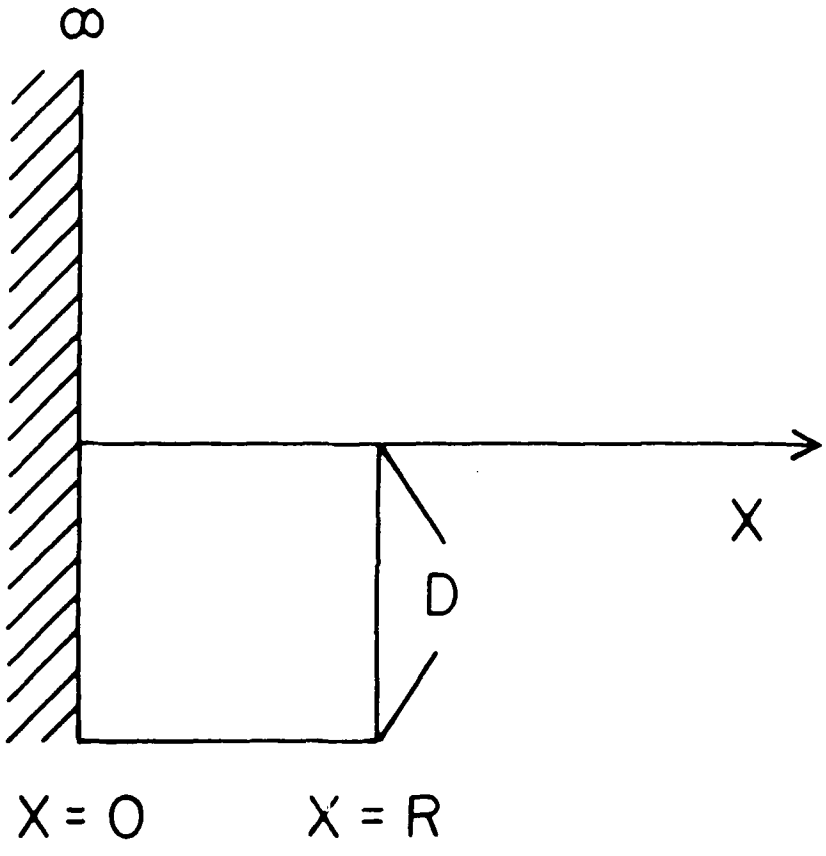

Fig. 2

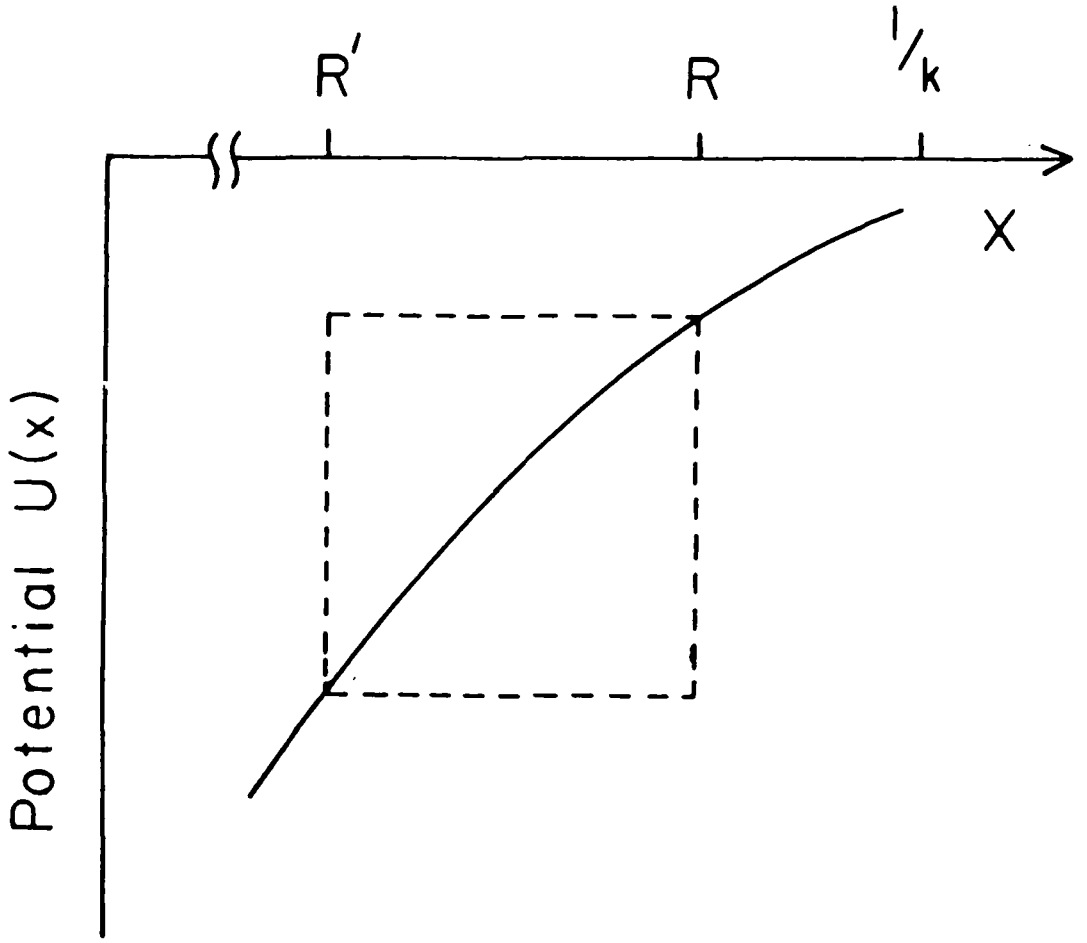

Fig. 3

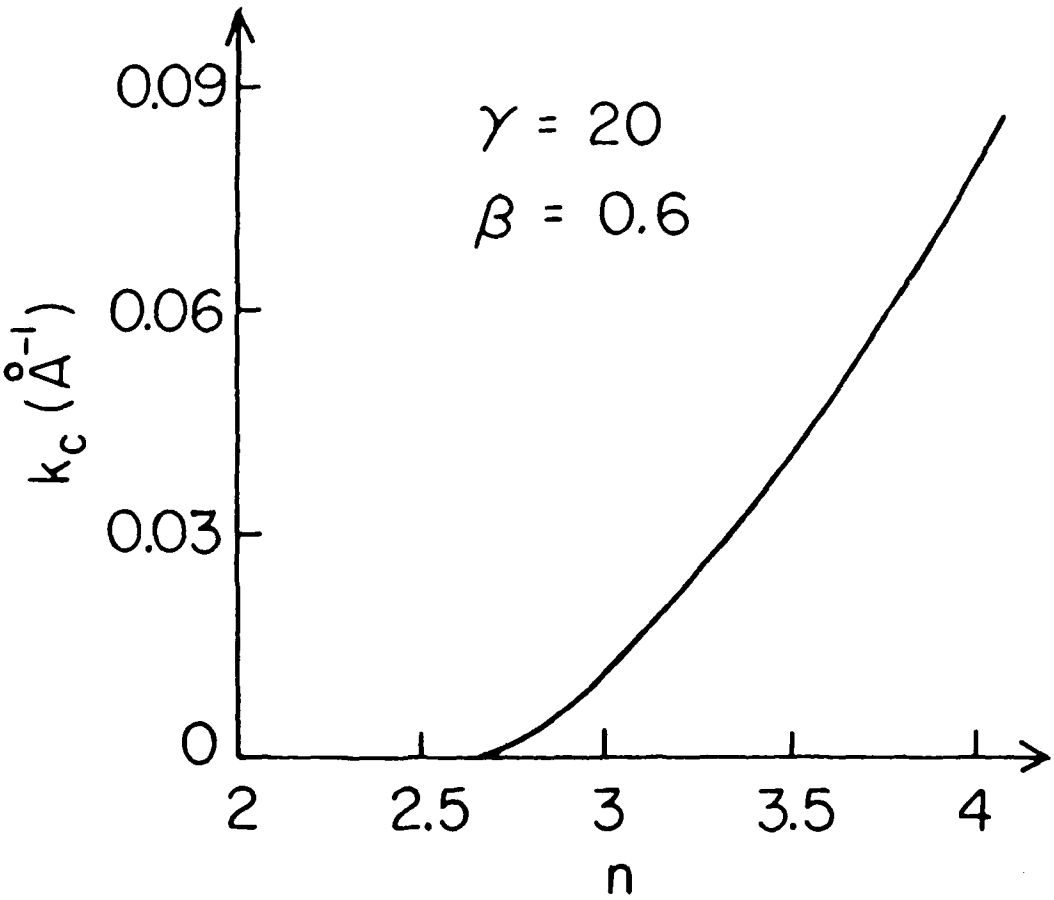

Fig. 4

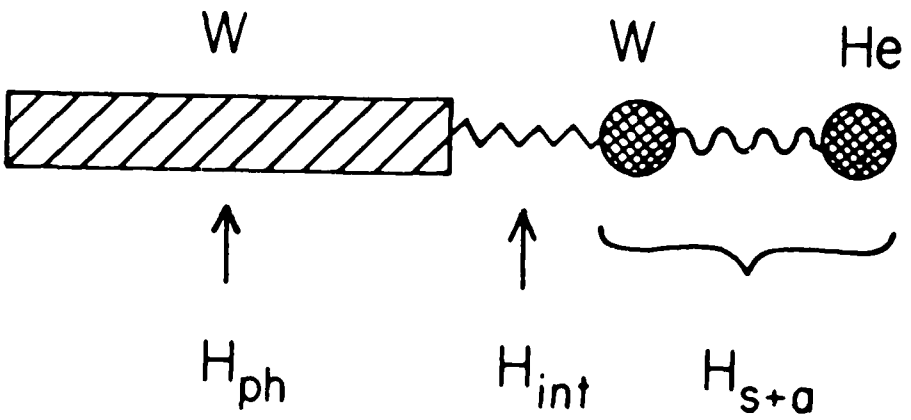

Fig. 5

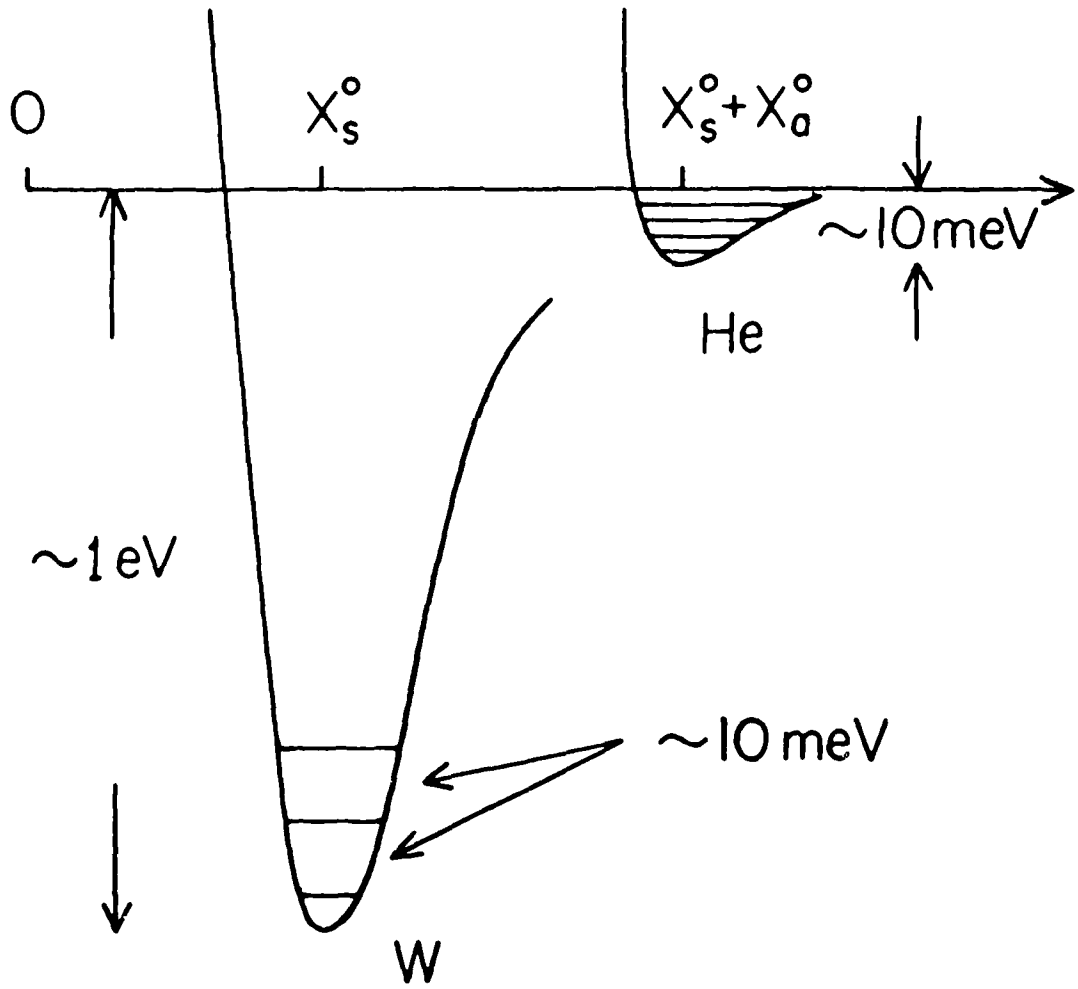

Fig. 6

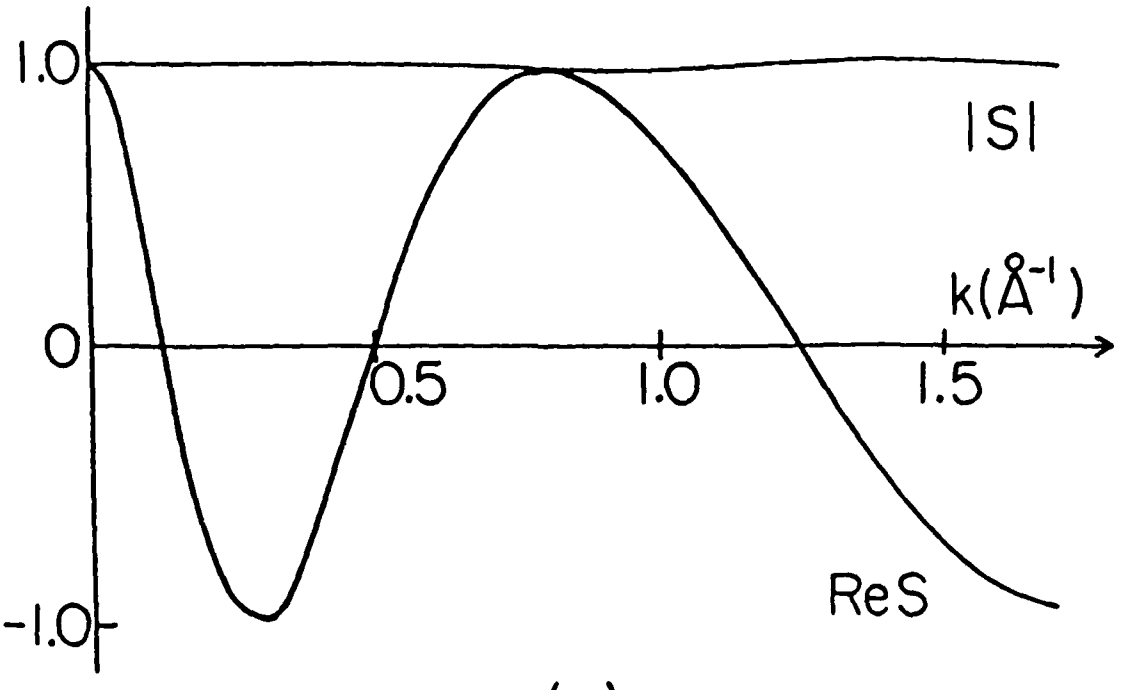

(a)

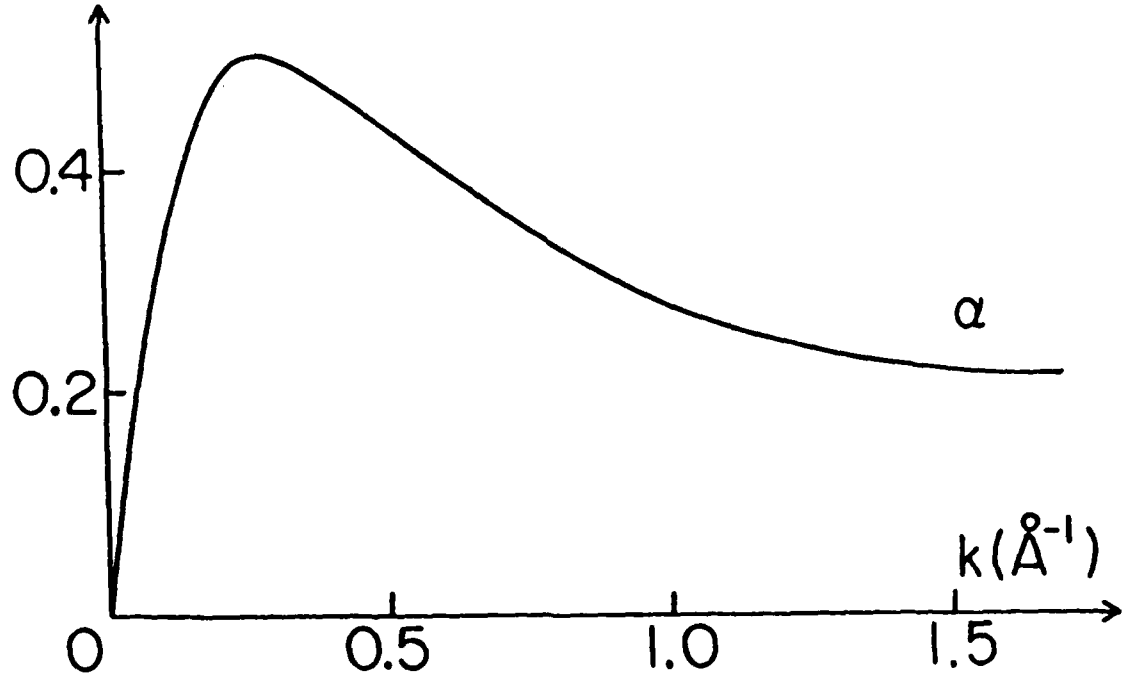

(b)

Fig. 7

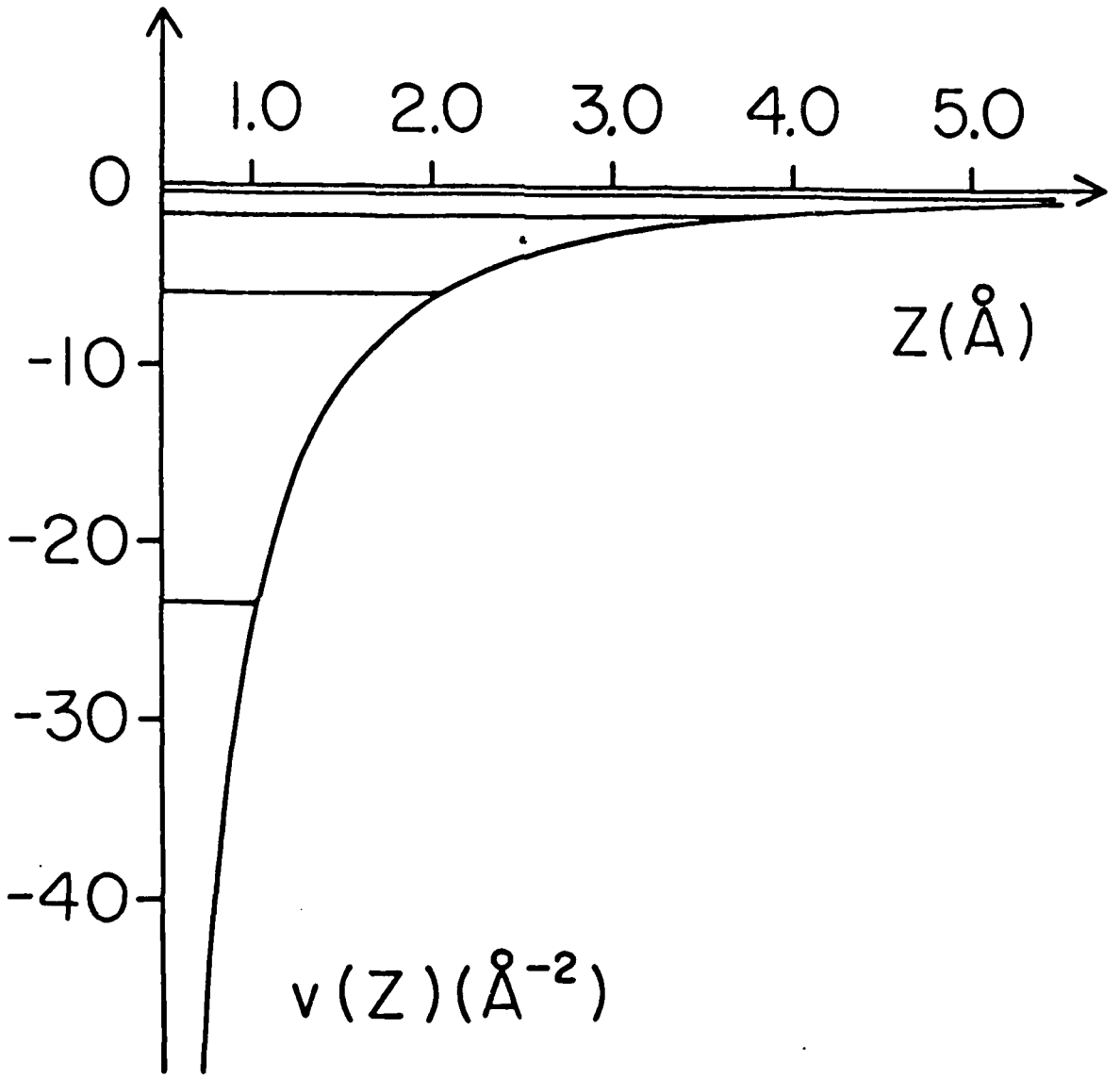

Fig. 8

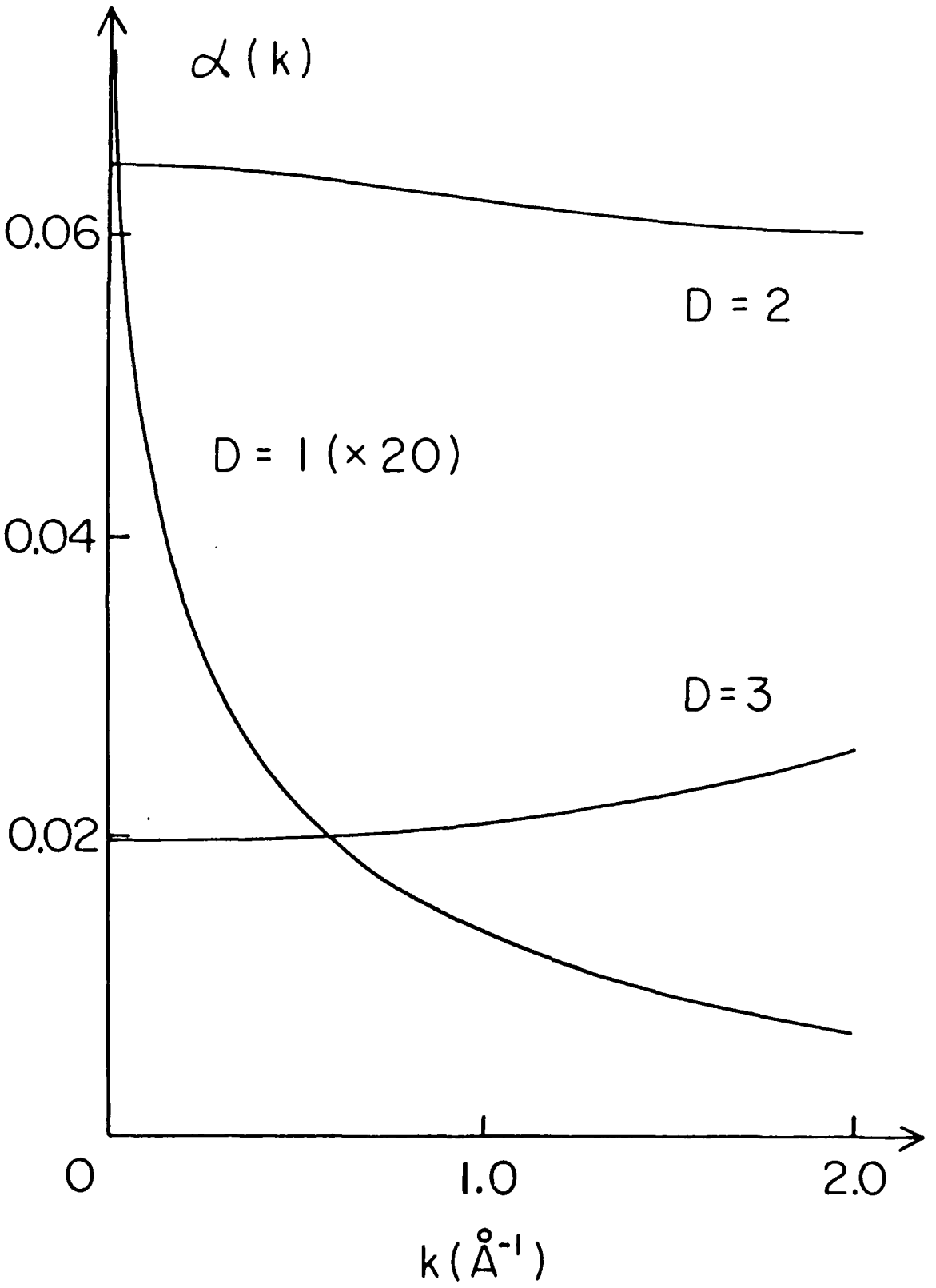

Fig. 9

TECHNICAL REPORT DISTRIBUTION LIST, GEN

	No. Copies
Office of Naval Research Attn: Code 1113 800 N. Quincy Street Arlington, Virginia 22217-5000	2
Dr. Bernard Douda Naval Weapons Support Center Code 50C Crane, Indiana 47522-5050	1
Naval Civil Engineering Laboratory Attn: Dr. R. W. Drisko, Code L52 Port Hueneme, California 93401	1
Defense Technical Information Center Building 5, Cameron Station Alexandria, Virginia 22314	12 high quality
DTNSRDC Attn: Dr. H. Singerman Applied Chemistry Division Annapolis, Maryland 21401	1
Dr. William Tolles Superintendent Chemistry Division, Code 6100 Naval Research Laboratory Washington, D.C. 20375-5000	1
Dr. David Young Code 334 NORDA NSTL, Mississippi 39529	1
Naval Weapons Center Attn: Dr. Ron Atkins Chemistry Division China Lake, California 93555	1
Scientific Advisor Commandant of the Marine Corps Code RD-1 Washington, D.C. 20380	1
U.S. Army Research Office Attn: CRD-AA-IP P.O. Box 12211 Research Triangle Park, NC 27709	1
Mr. John Boyle Materials Branch Naval Ship Engineering Center Philadelphia, Pennsylvania 19112	1
Naval Ocean Systems Center Attn: Dr. S. Yamamoto Marine Sciences Division San Diego, California 91232	1
Dr. David L. Nelson Chemistry Division Office of Naval Research 800 North Quincy Street Arlington, Virginia 22217	1

ABSTRACTS DISTRIBUTION LIST, 056/625/629

Dr. J. E. Jensen
Hughes Research Laboratory
3011 Malibu Canyon Road
Malibu, California 90265

Dr. J. H. Weaver
Department of Chemical Engineering
and Materials Science
University of Minnesota
Minneapolis, Minnesota 55455

Dr. A. Reisman
Microelectronics Center of North Carolina
Research Triangle Park, North Carolina
27709

Dr. M. Grunze
Laboratory for Surface Science and
Technology
University of Maine
Orono, Maine 04469

Dr. J. Butler
Naval Research Laboratory
Code 6115
Washington D.C. 20375-5000

Dr. L. Interante
Chemistry Department
Rensselaer Polytechnic Institute
Troy, New York 12181

Dr. Irvin Heard
Chemistry and Physics Department
Lincoln University
Lincoln University, Pennsylvania 19352

Dr. K.J. Klaubunde
Department of Chemistry
Kansas State University
Manhattan, Kansas 66506

Dr. C. B. Harris
Department of Chemistry
University of California
Berkeley, California 94720

Dr. F. Kutzler
Department of Chemistry
Box 5055
Tennessee Technological University
Cookesville, Tennessee 38501

Dr. D. DiLella
Chemistry Department
George Washington University
Washington D.C. 20052

Dr. R. Reeves
Chemistry Department
Renssaeler Polytechnic Institute
Troy, New York 12181

Dr. Steven M. George
Stanford University
Department of Chemistry
Stanford, CA 94305

Dr. Mark Johnson
Yale University
Department of Chemistry
New Haven, CT 06511-8118

Dr. W. Knauer
Hughes Research Laboratory
3011 Malibu Canyon Road
Malibu, California 90265

ABSTRACTS DISTRIBUTION LIST, 056/625/629

Dr. G. A. Somorjai
Department of Chemistry
University of California
Berkeley, California 94720

Dr. J. Murday
Naval Research Laboratory
Code 6170
Washington, D.C. 20375-5000

Dr. J. B. Hudson
Materials Division
Rensselaer Polytechnic Institute
Troy, New York 12181

Dr. Theodore E. Madey
Surface Chemistry Section
Department of Commerce
National Bureau of Standards
Washington, D.C. 20234

Dr. J. E. Demuth
IBM Corporation
Thomas J. Watson Research Center
P.O. Box 218
Yorktown Heights, New York 10598

Dr. M. G. Lagally
Department of Metallurgical
and Mining Engineering
University of Wisconsin
Madison, Wisconsin 53706

Dr. R. P. Van Duyne
Chemistry Department
Northwestern University
Evanston, Illinois 60637

Dr. J. M. White
Department of Chemistry
University of Texas
Austin, Texas 78712

Dr. D. E. Harrison
Department of Physics
Naval Postgraduate School
Monterey, California 93940

Dr. R. L. Park
Director, Center of Materials
Research
University of Maryland
College Park, Maryland 20742

Dr. W. T. Peria
Electrical Engineering Department
University of Minnesota
Minneapolis, Minnesota 55455

Dr. Keith H. Johnson
Department of Metallurgy and
Materials Science
Massachusetts Institute of Technology
Cambridge, Massachusetts 02139

Dr. S. Sibener
Department of Chemistry
James Franck Institute
5640 Ellis Avenue
Chicago, Illinois 60637

Dr. Arnold Green
Quantum Surface Dynamics Branch
Code 3817
Naval Weapons Center
China Lake, California 93555

Dr. A. Wold
Department of Chemistry
Brown University
Providence, Rhode Island 02912

Dr. S. L. Bernasek
Department of Chemistry
Princeton University
Princeton, New Jersey 08544

Dr. W. Kohn
Department of Physics
University of California, San Diego
La Jolla, California 92037

ABSTRACTS DISTRIBUTION LIST, 056/625/629

Dr. F. Carter
Code 6170
Naval Research Laboratory
Washington, D.C. 20375-5000

Dr. Richard Colton
Code 6170
Naval Research Laboratory
Washington, D.C. 20375-5000

Dr. Dan Pierce
National Bureau of Standards
Optical Physics Division
Washington, D.C. 20234

Dr. R. Stanley Williams
Department of Chemistry
University of California
Los Angeles, California 90024

Dr. R. P. Messmer
Materials Characterization Lab.
General Electric Company
Schenectady, New York 22217

Dr. Robert Gomer
Department of Chemistry
James Franck Institute
5640 Ellis Avenue
Chicago, Illinois 60637

Dr. Ronald Lee
R301
Naval Surface Weapons Center
White Oak
Silver Spring, Maryland 20910

Dr. Paul Schoen
Code 6190
Naval Research Laboratory
Washington, D.C. 20375-5000

Dr. John T. Yates
Department of Chemistry
University of Pittsburgh
Pittsburgh, Pennsylvania 15260

Dr. Richard Greene
Code 5230
Naval Research Laboratory
Washington, D.C. 20375-5000

Dr. L. Kesmodel
Department of Physics
Indiana University
Bloomington, Indiana 47403

Dr. K. C. Janda
University of Pittsburg
Chemistry Building
Pittsburg, PA 15260

Dr. E. A. Irene
Department of Chemistry
University of North Carolina
Chapel Hill, North Carolina 27514

Dr. Adam Heller
Bell Laboratories
Murray Hill, New Jersey 07974

Dr. Martin Fleischmann
Department of Chemistry
University of Southampton
Southampton 509 5NH
UNITED KINGDOM

Dr. H. Tachikawa
Chemistry Department
Jackson State University
Jackson, Mississippi 39217

Dr. John W. Wilkins
Cornell University
Laboratory of Atomic and
Solid State Physics
Ithaca, New York 14853

ABSTRACTS DISTRIBUTION LIST, 056/625/629

Dr. R. G. Wallis
Department of Physics
University of California
Irvine, California 92664

Dr. D. Ramaker
Chemistry Department
George Washington University
Washington, D.C. 20052

Dr. J. C. Hemminger
Chemistry Department
University of California
Irvine, California 92717

Dr. T. F. George
Chemistry Department
University of Rochester
Rochester, New York 14627

Dr. G. Rubloff
IBM
Thomas J. Watson Research Center
P.O. Box 218
Yorktown Heights, New York 10598

Dr. Horia Metiu
Chemistry Department
University of California
Santa Barbara, California 93106

Dr. W. Goddard
Department of Chemistry and Chemical
Engineering
California Institute of Technology
Pasadena, California 91125

Dr. P. Hansma
Department of Physics
University of California
Santa Barbara, California 93106

Dr. J. Baldeschwieler
Department of Chemistry and
Chemical Engineering
California Institute of Technology
Pasadena, California 91125

Dr. J. T. Keiser
Department of Chemistry
University of Richmond
Richmond, Virginia 23173

Dr. R. W. Plummer
Department of Physics
University of Pennsylvania
Philadelphia, Pennsylvania 19104

Dr. E. Yeager
Department of Chemistry
Case Western Reserve University
Cleveland, Ohio 41106

Dr. N. Winograd
Department of Chemistry
Pennsylvania State University
University Park, Pennsylvania 16802

Dr. Roald Hoffmann
Department of Chemistry
Cornell University
Ithaca, New York 14853

Dr. A. Steckl
Department of Electrical and
Systems Engineering
Rensselaer Polytechnic Institute
Troy, NewYork 12181

Dr. G.H. Morrison
Department of Chemistry
Cornell University
Ithaca, New York 14853

END

12-87

DTIC